THE COEFFECTS OF VITAMIN B_{12} AND IRON ON MARINE DIATOMS

Kelsey Ellis

A thesis submitted to the faculty at the University of North Carolina at Chapel Hill in partial fulfillment of the requirements for the degree of Master of Science in the Marine Sciences Department in the College of Arts and Sciences.

Chapel Hill
2015

Approved by:

Adrian Marchetti

Marc Alperin

Andreas Teske

ABSTRACT

Kelsey Ellis: The effects of vitamin B_{12} and iron on marine diatoms
(Under the direction of Adrian Marchetti)

Pseudo-nitzschia and *Fragilariopsis* are two closely related marine diatoms, yet *Pseudo-nitzschia* possess only the vitamin B_{12}-dependent form of the methionine synthase enzyme [MetH] whereas *Fragilariopsis* possess both MetH and a B_{12}-independent form [MetE]. Consistent with this difference in gene repertoires, our results indicate that *Pseudo-nitzschia granii* has an obligate requirement for vitamin B_{12} while growth of *Fragilariopsis cylindrus* was unaffected by varying B_{12} availability due to increased MetE expression.

Iron and vitamin B_{12} can be colimiting in marine high-nutrient, low-chlorophyll [HNLC] regions. Understanding how variations in these nutrients affect diatom growth can further elucidate community succession dynamics in these areas. Our study, conducted with B_{12}-requiring *Pseudo-nitzschia granii* and MetE-possessing *Grammonema cf. islandica*, showed that the effects of Fe-B_{12} colimitation are not synergistic, but rather that Fe effects dominate physiological measures of diatom health regardless of whether a diatom is auxotrophic for vitamin B_{12}.

ACKNOWLEDGMENTS

I'd like to thank my advisor, Adrian Marchetti, for letting me volunteer in his lab as an undergraduate even though I knew nothing about diatoms or molecular biology—who would've thought back then that I'd someday be writing a Master's thesis! I'd also like to thank all the members of the Marchetti lab, past and present, for always being there for me. Special thanks to Natalie Cohen, Wilton Burns, and Carly Moreno for keeping me from going crazy during long days and late nights in the lab. And, last but not least, I'd like to thank my diatoms: through the good times and the bad, we've grown together.

TABLE OF CONTENTS

LIST OF TABLES

LIST OF FIGURES

LIST OF ABBRREVIATIONS

ACT	Actin gene
AT	antibiotic-treated
Chl *a*	chlorophyll *a*
dNTP	deoxynucleoside triphosphate
Fe	iron
HNLC	high-nutrient, low chlorophyll
LB media	Luria Broth media
MetH	B_{12}-dependent methionine synthase
MetE	B_{12}-independent methionine synthase
TMC	trace-metal clean

INTRODUCTION

Although diatoms are microscopic, their primary production is estimated to be responsible for 20% of global carbon fixation each year. In addition, they create as much as 40% of annual marine organic carbon (Armbrust et al. 2004, Nelson et al. 1995). Over geologic timescales, it is hypothesized that changing rates of carbon sequestration into the deep ocean due to changes in diatom growth have influenced climate on a global scale (Brzezinski et al. 2002).

The growth rate and ecological success of diatoms is dependent on whether they receive enough nutrients to fuel photosynthesis and carbon fixation. For many years, researchers focused on the role of macronutrients such as nitrate, phosphate, and silicate on limiting diatom growth in the world's oceans (Gobler et al. 2007). However, recent studies have shown that micronutrients such as iron [Fe] are scarce enough to limit primary production in vast areas of the ocean, called high-nutrient, low-chlorophyll (HNLC) areas (de Baar et al. 2005). These areas comprise approximately 30% of the ocean's surface and include the Southern Ocean, Equatorial Pacific, and Northeast Pacific Ocean (Boyd et al. 2007).

Research has also shown that cobalamin, or vitamin B_{12}, can be limiting or colimiting with Fe in HNLC areas as well as other marine environments (Bertrand and Saito 2007, Gobler et al. 2007, Koch et al. 2011). Vitamin B_{12} has been shown to be a factor capable of affecting phytoplankton growth in areas such as the Ross Sea (Bertrand et al. 2007), the Southern Ocean (Panzeca et al. 2006), near Long Island (Sañudo-Wilhelmy et al. 2006), the Sargasso Sea (Menzel and Spaeth 1962), and the Gulf of Maine (Swift 1981).

Incorporating the Fe and B_{12} effects into the traditional "Redfield ratio" has proved complicated due to a number of factors. These factors include complex Fe and B_{12} speciation, diverse requirements among phytoplankton species, and the role these micronutrients play in altering the uptake of classical 'Redfield' nutrients (Eppley and Peterson 1979). In addition, the potential for biochemical interactions between Fe and B_{12}, both at a cellular and an ecosystem level, are not well understood.

This thesis aims to examine the role vitamin B_{12} dynamics play in areas of the ocean where the vitamin may be limiting (Chapter 1) or colimiting (Chapter 2) with Fe. In Chapter 1, we will determine whether survival under B_{12} limitation correlates with the presence of a B_{12}-independent enzyme isoform [MetE] in a diatom's gene repertoire, and examine the potential for biogeographical variations in MetE presence. In Chapter 2, we aim to determine how iron colimitation and fertilization affect this dynamic, at both the physiological and molecular level. By pairing physiological measurements with gene expression analysis, we can gain a better understanding of how differences at the molecular level can translate into large scale changes in diatom bloom formation that have the potential to affect processes such as carbon sequestration, biogeochemical cycling, and microbial community dynamics.

CHAPTER 1: THE EFFECTS OF VITAMIN B_{12} ON BLOOM-FORMING DIATOMS

Introduction

Vitamin B_{12}, or cobalamin, is a cobalt-containing organometallic molecule that is synthesized by certain archaea and bacteria, including cyanobacteria (Bertrand et al. 2007, Bonnet et al. 2010). Its biological importance lies in the role as a cofactor in one form of the methionine synthase enzyme [MetH] which catalyzes the synthesis of the amino acid methionine and is present in all examined marine eukaryotic microalgae (Banerjee and Matthews 1990, Helliwell et al. 2011). Many of these algal species are B_{12} auxotrophs, meaning they have an obligate requirement for B_{12} and likely only possess the MetH gene (Croft et al. 2005). However, a cobalamin-independent methionine synthase [MetE] that does not require vitamin B_{12} to create methionine also exists in some algae, including certain diatom species.

Another B_{12}-dependent enzyme, methylmalonyl-CoA mutase, has been found in all examined Chromalveolate genomes, which include all diatom species (Helliwell et al. 2011). This enzyme requires the B_{12}-containing molecule adenosylcobalamin and may be used in fatty-acid utilization, among other metabolic activities. However, as this enzyme is found in diatoms that do not require B_{12}, it is not the primary determinant of B_{12} auxotrophy (Croft et al. 2006). Instead, there is a strong correlation between an absence of a functional MetE gene and B_{12} auxotrophy among examined microalgae (Helliwell et al. 2011).

Both forms of methionine synthase catalyze the conversion of homocysteine and methyl-tetrahydrofolate to tetrahydrofolate and methionine, although the exact pathway is less well elucidated for the MetE enzyme (Bertrand and Allen 2012). Despite functional similarity, MetE

and MetH are unrelated both in sequence homology and protein folding structure (Pejchal and Ludwig 2005). In addition, MetE is approximately 100-fold less catalytically efficient than MetH, with significantly slower observed turnover times for the enzyme (González et al. 1992). This inefficiency results in 30-40 fold increases in the nitrogen and zinc requirements allocated to MetE activity over what is used for MetH (Bertrand et al. 2013).

Although the only currently known determinant of whether MetH or MetE is utilized is vitamin B_{12} availability, these genomic alterations can have ecosystem-scale implications. Until recently, research in high-nutrient, low-chlorophyll [HNLC] regions of the world's oceans focused primarily on the role of Fe limitation in sustaining low primary production despite high concentrations of macronutrients. Iron fertilization experiments have subsequently shown that these regions are limited by bioavailable Fe and fertilization of HNLC waters with Fe creates diatom-dominated phytoplankton blooms (de Baar et al. 2005, Boyd et al. 2007) that have the potential to sequester large amounts of carbon in seafloor sediments (Smetacek et al. 2012). More recent investigations in Fe-limited regions of the ocean have shown that in some cases, by adding both vitamins and Fe, diatom growth can be enhanced beyond that of Fe enrichment alone. In particular, vitamin B_{12} is capable of increasing growth with or without Fe under certain environmental conditions in HNLC regions (Panzeca et al. 2006, Bertrand et al. 2007, Koch et al. 2011). Vitamin B_{12} is also capable of affecting phytoplankton growth and community structure in coastal and estuarine waters (Sañudo-Wilhelmy et al. 2006, Gobler et al. 2007, Koch et al. 2011).

The biosynthesis of vitamin B_{12} by marine prokaryotes affects oceanic B_{12} distributions, as these organisms are the sole source of the vitamin to eukaryotic algae, including diatoms (Croft et al. 2005). Phytoplankton may acquire the vitamin from dissolved B_{12} released through

excretion, cell lysis, and direct symbiotic interactions with bacteria and archaea (Droop 2007, Bonnet et al. 2010, Kazamia et al. 2012). Therefore, an important determinant of vitamin B_{12} distribution is the abundance and composition of marine bacterial and archaeal communities. In addition, diatoms without MetE may compete with other B_{12}-auxotrophic algae and bacteria when vitamin concentrations are low.

Specific bacterial genera, namely *Sulfitobacter*, *Roseobacter*, *Alteromonas*, and *Flavobacterium*, have reoccurred as predominant groups in diatom-bacteria association studies (Grossart et al 2005, Kaczmarska et al. 2005, Amin et al. 2012). In addition, whole-genome sequencing has thus far shown that *Cyanobacteria, Thaumarchaea,* and members of *Alphaproteobacteria*, such as *Magnetococcales*, *Rhizobiales*, and *Rhodobacterales*, are the main marine B_{12}-synthesizers (Doxey et al. 2014, Sañudo-Wilhelmy et al. 2014). The cellular requirements leading to B_{12} limitation have ecological effects, since diatoms possessing MetE can forgo the requirement for B_{12} and thus reduce their dependency on B_{12}-producing bacteria. This allows diatoms with MetE to potentially decrease their dependence on B_{12}-producing bacteria in a way that auxotrophic species cannot.

Recent phylogenetic analysis of MetE sequences among diverse algal groups indicates that multiple independent gene losses are likely the mechanism behind widespread but randomly distributed B_{12} auxotrophy. The discovery of MetE unitary pseudogenes in multiple algal species corroborates this theory (Helliwell et al. 2011, 2013). Although many diatom species have an obligate requirement for B_{12}, the phylogenetic patterns among diatom species possessing MetE was previously difficult to examine due to a scarcity of genomic information. The primary objective of this study was to investigate whether variations in B_{12}-related gene repertoires among ecologically important marine diatom species may determine B_{12} auxotrophy and thus

affect large scale processes such as community succession and carbon sequestration in areas with variable vitamin supply.

Methods

Algal species

Isolates of six diatom species were examined during this study (Table 1.1).

			Transcriptome	
Diatom	Strain	18S Accession ID	Database	Organism ID
F. kerguelensis	L26-C5	KJ866919	MMETSP	733
F. cylindrus	CCMP1102	AY485467	JGI	272258
P. granii	UNC1102	KJ866907	SRA	SRR290905
Chaetoceros sp.	UNC1201	KJ866910	MMETSP	1429
Skeletonema sp.	UNC1202	KJ866908	MMETSP	1428
Thalassiosira sp.	UNC1203	KJ866909	NA	NA
Grammonema cf. islandica	UBC1301	AJ535190	NA	NA

Table 1.1. Identification information for diatom species examined in this study (Chapter 1 and Chapter 2).

Pseudo-nitzschia granii (UNC1102) (G.R. Hasle) was obtained from Ocean Station Papa (50°00 N, 145°00 W) in the Northeast Pacific Ocean in 2010 (18S Genbank accession number KJ866907), *Fragilariopsis cylindrus* (CCMP1102) (Grunow) was obtained from the Provasoli-Guillard National Center for Marine Algae and Microbiota (NCMA) and originally isolated from the Indian Ocean sector of the Southern Ocean in 1979 (64°04 S, 48°42), *Fragilariopsis kerguelensis* (O'Meara) was obtained from the Atlantic sector of the Southern Ocean (48°00 S, 16°00 W) in 2009 (18S Genbank accession number KJ866919), and *Thalassiosira* sp.

(UNC1203) (Cleve), *Skeletonema* sp. (UNC1201) (Greville) and *Chaetoceros* sp. (UNC1202) (Ehrenburg) were obtained from the Northeast Pacific Ocean (48°49 N, 128°40 W) in 2012 (18S Genbank accession numbers KJ866909, KJ866908, and KJ866910, respectively). Based on rDNA (ribosomal deoxyribonucleic acid) 18S sequencing, the *Thalassiosira* sp. UNC1203 isolate shares 99% homology to sequences to both *Thalassiosira aestivalis* and *Thalassiosira nordenskioeldii* deposited in Genbank. The *Skeletonema* sp. UNC1201 rDNA 18S sequence matches both *Skeletonema marinoi* and *Skeletonema dohrnii*, as these two species have been found to be indistinguishable based on 18S rDNA analysis (Kooistra et al. 2008). The *Chaetoceros* sp. UNC1202 isolate is 93% homologous to *Chaetoceros gracilis*. Due to present ambiguities in identifications of the centric diatom isolates to the species level, only genus names are used throughout this study. Genbank accession numbers for MetH are indicated in Figure 1.5, while those for MetE are listed in Appendix 2.

Medium and culture conditions

All phytoplankton cultures were grown in artificial seawater medium [Aquil] using trace metal clean [TMC] techniques as according to Marchetti et al. (2006). Macronutrients were added to Aquil medium in final concentrations of 300 μmol L^{-1} NO_3, 10 μmol L^{-1} PO_4, and 100 μmol L^{-1} $Si(OH)_4$ to achieve macronutrient-replete growth. All dispensing of medium occurred under a positive-pressure, laminar-flow hood. Before use, Aquil medium was microwaved in a 2-L Teflon bottle for sterilization. Medium was dispensed into 2-L acid-cleaned, milli-Q H_2O-rinsed polycarbonate bottles and supplemented with filter-sterilized (0.2-μm Acrodisc) Fe, ethylenediamine tetraacetic acid [EDTA] trace metals, and vitamins (thiamine and biotin) according to Aquil medium concentrations (Price et al. 1988/89). Pre-filtered vitamin B_{12} was

added so that its concentration in the medium was $5.5 \cdot 10^{-7}$ kg m^{-3} (405 pmol L^{-1}) for a B_{12}-replete treatment [+B_{12}], or was excluded altogether to create B_{12}-absent medium [-B_{12}] while all other additions were made in excess concentrations. Trace-metal concentrations were buffered using 100 µmol L^{-1} of EDTA. Premixed Fe-EDTA (1:1) was added at total concentrations of 1.37 µmol L^{-1} to achieve free ferric-ion concentrations 10^{-19} mol L^{-1} [pFe 19], which was considered to be Fe-replete medium. The Aquil medium was allowed to chemically equilibrate overnight before use and was stored in a TMC room.

Phytoplankton cultures were grown and maintained in acid-washed, 28-mL polycarbonate centrifuge tubes at 12°C (*P. granii*, *Thalassiosira* sp. UNC1203, *Skeletonema* sp. UNC1201 and *Chaetoceros* sp. UNC1202) or 4°C (*F. cylindrus* and *F. kerguelensis*). Cultures were grown on rotator tables under a continuous, saturating photon flux density of 120-150 µmol photons m^{-2} s^{-1}, using the semicontinuous batch culture technique described by Brand et al. (1981). Cultures were grown until late exponential phase, upon which a 50 µL subaliquot of culture was transferred into fresh medium. Each of the studied diatom species were grown under +B_{12} and -B_{12} conditions, both in the presence of their full bacterial assemblage and after antibiotic treatment (AT), except *F. kerguelensis* which was grown under non-AT conditions only. Growth rates and photosynthetic efficiencies (F_v/F_m) were measured for each diatom species under the different treatments. Duplicate cultures were maintained for +/- B_{12} treatments.

Phytoplankton growth was estimated by directly measuring in vivo fluorescence using a Turner Designs model 10-AU fluorometer (in vivo chlorophyll optical kit) after confirming a proportional relationship between fluorescence and cell concentration. The r^2 value of in vivo fluorescence versus cell concentration standard curve for *P. granii* for both +B_{12} and -B_{12} treatments was >0.92 (n = 12, data not shown). Specific growth rates were calculated from the

slope of a linear regression of the natural log of in vivo fluorescence versus time during the exponential growth phase of acclimated cells after 3 successive transfers in +/- B_{12} medium. Cells were considered acclimated when growth rates did not vary by >10%, which typically required 3-4 transfers in $+B_{12}$ or $-B_{12}$ medium. If culture growth ceased during that time and responded positively to an addition of vitamin B_{12}, cells were characterized as being unable to grow in the absence of vitamin B_{12}.

The response of photosynthetic efficiency [F_v/F_m] to variations in vitamin B_{12} concentrations was measured from fluorescence-induction measurements performed on cells in mid-exponential phase using a Satlantic FIRe Fluorometer. Before each measurement, a subsample (5 mL) of each culture was placed in the dark for 20 minutes. A strong short pulse of high luminosity blue light was applied to dark-acclimated phytoplankton for 80 μs duration to cumulatively saturate PSII and measure fluorescence induction from minimum [F_o] to maximum [F_m] fluorescence yields. After the subtraction of a blank of Aquil medium, maximum quantum yield [F_v/F_m] of PSII was calculated. The PSII quantum yield Y was quantified by $Y = F_v/F_m$ ($F_v = F_m - F_o$) (Kitajima and Butler 1975).

Sterile techniques were used for all cultures to minimize bacterial contamination and the AT cultures were created by adding a mixture of antibiotics to 5 mL of an exponentially growing culture for 24 hours. Final concentrations of antibiotics were 50 μg mL^{-1} strepomycin, 66.6 μg mL^{-1} gentamycin, 20 μg mL^{-1} ciprofloxacin, 2.2 μg mL^{-1} chloramphincol (in ethanol), and 100 μg mL^{-1} ampicillin. A 5-mL algal culture with the appropriate antibiotic concentrations was incubated for 24 hours before a 1-mL aliquot was transferred into fresh sterile Aquil medium of the corresponding treatment (+/-B_{12}). After 2-3 transfers in AT conditions, the cultures were examined periodically for bacterial contamination using the bacteriological peptone marine broth

test and through SYBR staining and examination of the culture using epifluorescent microscopy (Noble and Fuhrman 1998). The reduction in bacteria was quantified by performing cell counts using Olympus Metamorph Basic (v.7.6.0.0) software's integrated morphometry analysis on 10 randomly chosen fields of view from each SYBR-stained filter, which were then averaged. In all AT cultures, bacterial abundances were substantially reduced (93-99% reduction in all cultures) after incubation with antibiotics (Appendix 3).

B_{12} Addback Experiments

In addition to measuring steady-state growth rates, changes in growth and gene expression in response to variation in vitamin B_{12} concentrations were measured for *P. granii* and *F. cylindrus* by growing cultures under non-AT +/- B_{12} conditions and performing an addback of vitamin B_{12} to the growth medium. Cultures were grown under similar conditions as described above in modified TMC, 2-L polycarbonate bottles with Teflon tubing to permit subsampling with minimum contamination. All subsampling was performed under a positive-pressure, laminar-flow hood. A Teflon stir bar was added to each experiment and the culture was incubated on top of a stir plate to ensure the culture remained well mixed. Aquil medium was prepared using the same methodology as described previously and inoculated from respective steady-state growth cultures (either $+B_{12}$ or $-B_{12}$). All experiments were inoculated when steady-state cultures were in mid-exponential growth phase and, except in the case of *P. granii* $-B_{12}$ treatments, cultures were transferred into the same treatment they were previously acclimated to. Because *P.granii* growth ceased after approximately 2 transfers in $-B_{12}$ medium in both non-AT and AT cultures, previously $+B_{12}$ *P.granii* were inoculated into $-B_{12}$ medium, grown to mid-exponential phase within a 28-mL centrifuge tube, and transferred into 2-L bottles containing 1 L

–B_{12} medium for experimental growth measurements. Fluorescence measurements of subsamples were taken from each culture 1-2 times each day. F_v/F_m measurements were performed using the same methodology described above. The length of experiments varied among diatom species and experimental treatments, but was typically between 5-10 days.

When fluorescence measurements indicated that cultures were in late exponential growth phase, 5-mL aliquots were taken for F_v/F_m and fluorescence measurements. 600 mL of each culture was filtered onto a 3.0-μm polycarbonate filter, immediately frozen in liquid nitrogen, and stored at -80°C until RNA extraction.

After this initial sampling time point, 400 μl of vitamin B_{12} (405 pmol L^{-1}) was added to each experiment regardless of prior B_{12} concentration. Initial –B_{12} cultures then had a B_{12} concentration of 405 pmol L^{-1} and +B_{12} cultures were >405 pmol L^{-1}. This was done to ensure that the response of initial +B_{12} cultures acted as a control, showing whether the addition procedure itself would influence growth and gene expression regardless of initial treatment. Both concentrations are well above those needed to achieve B_{12}-replete growth of the diatom cultures. Cultures were then incubated for an additional 24 hours before the same set of filtrations were repeated, with the exception of the volume filtered for RNA being reduced to 200 mL due to higher cell densities.

Gene expression analysis

Primers for qPCR were developed using Primer 3 and tested using PCR, gel electrophoresis, and PCR product sequencing (Appendix 1). RNA was extracted from thawed samples using the RNAqueous-4PCR extraction kit (Invitrogen) according to the manufacturer's protocols. The RNA was then incubated with deoxyribonuclease [DNase] I at 37°C for 45

minutes and purified by DNase inactivation reagent. RNA concentrations were measured using a Nanodrop spectrophotometer and samples with concentrations <250 ng/µl were concentrated using the RNeasy MinElute Cleanup Kit (Qiagen, Hilden, Germany). qPCR runs using the RNA samples were used to determine DNA contamination levels, with samples containing >10 DNA copies per □L of RNA given an additional incubation with DNase I and purified once more. Two µg of each RNA sample was reverse transcribed into cDNA using Superscript III First Strand Synthesis Systems for reverse transcription quantitative polymerase chain reaction (RT-qPCR; Invitrogen, NY, USA). cDNA aliquots were diluted with water to obtain 60 µL total for each sample prior to use in qPCR.

The number of transcript copies of each gene of interest was quantified by qPCR in triplicate 20-µL reactions composed of 2 µL DNA standard or cDNA unknown, 10 µL Kapa SyberFast Universal qPCR Kit (Kapa, MA, USA), and 1.6 µL of both forward and reverse primers. qPCR was run on an Eppendorf Mastercycler ep realplex. A dilution series of standards was run at the same time as experimental unknowns. Gene standards for qPCR were created by PCR amplification at 94°C for 2 minutes, followed by 40 cycles of 30 seconds at 95°C, 30 seconds at the specific primer's annealing temperature, and 1 minute at 72°C. Reactions consisted of 1 µL DNA, 1 µL Taq Buffer, 1 µL $MgCl_2$, 0.5 µL dNTP, 0.4 µL of forward and reverse primers, 0.075 µL Taq polymerase, and 4.625 µL UV-light treated water. Amplified fragments were cloned and transformed into *Escherichia coli* using the TOPO TA Cloning Kit (Invitrogen). Colonies containing the cloned gene fragment were incubated at 37°C overnight in liquid Luria broth [LB] media, and plasmids were extracted using QIAprep Spin Miniprep Kit (Qiagen, Hilden, Germany). Plasmids were linearized through incubation with *SpeI* at 37°C for 1 hour and enzyme denaturation at 80°C for 20 minutes. Linearized plasmids were quantified on a

Qubit using the Qubit RNA Assay Kit (Invitrogen, NY, USA) and the copy number per microliter was calculated. Serial dilutions with UV-light treated water were used to create a series of standards for each gene of interest (10^6, 10^5, 10^4, 10^3, 10^2, 10^1 copies/μL). Transcript copy numbers were normalized to Actin [ACT] copy numbers from the same cDNA sample. The Actin gene was used as a "housekeeping" gene for both *P. granii* and *F. cylindrus* and is a commonly-used housekeeping gene that remains stable under a variety of nutrient regimes (Alexander et al. 2012).

Phylogenetic Analysis

Sequences for genes examined in this study (i.e. MetH, MetE and ACT) from diatoms with whole genomes publically available (e.g. *F. cylindrus*) were obtained from Joint Genome Institute's genome portals. *P. granii* sequences for MetH and ACT were obtained from an Expressed Sequence Tag (EST) library performed as part of a previous study (Marchetti et al. 2012) that is deposited in NCBI's Sequence Read Archive (SRA) (accession number SRX066541). Seven recently sequenced transcriptomes from Southern Ocean polar diatom isolates were also used in the phylogenetic analysis of MetH and MetE (C.Moreno unpubl. data). Remaining diatom sequences were obtained from transcriptomes of isolates sequenced as part of the Marine Microbial Eukaryote Transcriptome Sequencing Project (MMETSP) and deposited in SRA (Bioproject accession number PRJNA231566) and the CAMERA database (CAM_P_0001000). All sequences were identified through a search for homologous sequences using BLASTp (v. 2.2.28) with an e-value threshold of $<10^{-5}$. Locations of MMETSP isolates were obtained from the MMETSP metafile available on CAMERA and information gathered from culture collection websites (Appendix 4).

MetE homologs from diatom species within the MMETSP database were identified through sequence homology searches against the *F. cylindrus* MetE protein sequence (Appendix 1). Among the diatom species in which MetE was identified, paired aligned transcript copies ranged from 4 (*Chaetoceros sp*. UNC1202) to 1673 (*Staurosira complex sp*.) suggesting sequencing depth within each of these diatom transcriptomes was sufficient for initial screening of MetE distributions (Appendix 2). However, because gene expression can vary according to changes in growth conditions, the absence of a MetE homolog should not definitively be taken as evidence that the gene is not present within the genome of an isolate. Since the cultures used in this phylogenetic analysis were not grown under B_{12}-limited conditions, there is the possibility that MetE could be present but not identified in the process of transcriptome sequencing.

Translated MetH and MetE sequences were separately aligned using MUSCLE (Edgar 2004) within MEGA (version 6; Tamura et al. 2013). MMETSP contigs shorter than 800 amino acids long in the case of MetH, and 600 in the case of MetE, were excluded to obtain an alignment that spanned the majority of the genes. MetE sequences larger than 1,500 were trimmed to under 1,000 after an initial MUSCLE alignment with the F. cylindrus MetE genome sequence. A phylogenetic tree of marine microbial eukaryotic organisms possessing MetE was created using the Maximum Likelihood method with the LG+G substitution model, partial deletion of residues and resampling with one hundred bootstrap replicates. Included isolates were then grouped according to Parfrey et al. 2010 and Dorrell and Smith 2011 into eukaryotic "supergroups." A MetH tree of diatom species was created using the same methodology, with the exception of the usage of the LG+G+I substitution model and grouping according to class as raphid pennates, araphid pennates, radial centrics, or bi(multi)polar centrics according to Sorhannus 2007. Diatom species with either full or partial sequence of an identifiable MetE gene

according to MMETSP BLAST results against the known *F. cylindrus* genome MetE gene are indicated on the MetH phylogenetic tree.

A map showing the distribution of sequenced diatom isolates with MetE compared to those without a BLAST hit for the gene was created by C. Moreno.

Statistical Analyses

To test for significant differences between treatments, two-tailed homoscedastic t-tests within each species were performed on steady-state culture growth rate data. Two-tailed homoscedastic t-tests were also performed to test for significant differences between F_v/F_m values between treatments. A two-tailed pairwise t-test was performed between the pre $+B_{12}$ and pre $-B_{12}$ F_v/Fm values for the B_{12} addback experiments.

To test for significant differences between ratios of gene expression pre and post B_{12} addback, two-tailed pairwise homoscedastic t-tests were performed on gene expression ratios from B_{12} addback experiments. To reduce technical error in pipetting or mixing, the standard deviation of the mean for each triplicate ratio measurement was <10% of the mean. The level of statistical significance for all tests was $p<0.05$. All tests were performed in Sigmaplot 12.5 and passed the Shapiro-Wilk Normality Test and Equal Variance Test unless otherwise stated, in which case the Mann-Whitney U-Statistic is used in place of a p-value.

Results

Steady-State Growth Rates and Photosynthetic Efficiencies

Determining growth rate differences between non-antibiotic-treated and antibiotic-treated (non-AT and AT) $+/-B_{12}$ treatments for *P. granii* and *Thalassiosira* sp. UNC1203 were not

possible as $-B_{12}$ cultures could not be maintained in steady state (Table 1.2). While *Chaetoceros* sp. UNC1202 $-B_{12}$ and AT $-B_{12}$ treatments did not cease growth completely, growth rates were significantly slower in $-B_{12}$ treatments (Mann-Whitney U Statistic = 3.5). Growth rates were also significantly different between *Chaetoceros* sp. UNC1202 $-B_{12}$ and AT $-B_{12}$ treatments ($p = 2.5\times10^{-5}$). *Skeletonema* sp. UNC1201 exhibited significantly slower growth between $+B_{12}$ and $-B_{12}$ treatments, and growth ceased in AT $-B_{12}$ treatments ($p = 3.10\times10^{-6}$). There were no significant differences between B_{12} treatments for *F. cylindrus* and *F. kerguelensis* for both non-AT and AT cultures.

Class	Diatom	MetE [a]	Antibiotic -Treated	B_{12} Status	Growth Rate (d^{-1})	n	F_v/F_m	n
raphid pennates	*F.cylindrus*	+	-	+	0.34 ± 0.02	9	0.68 ± 0.01	2
[Bacillariophyceae]		+	-	-	0.32 ± 0.08	10	0.67 ± 0.01	3
		+	+	+	0.37 ± 0.05	3	0.65 ± 0.01	3
		+	+	-	0.33 ± 0.04	3	0.64 ± 0.02	3
	F. kerguelensis	+	-	+	0.19 ± 0.02	4	na	
		+	-	-	0.19 ± 0.02	3	na	
		+	+	+	na		na	
		+	+	-	na		na	
	P. granii	-	-	+	1.02 ± 0.06	15	0.71 ± 0.006	3
		-	-	-	ng		ng	
		-	+	+	1.19 ± 0.2	3	0.71 ± 0.01	3
		-	+	-	ng		ng	
bi(multi)polar centrics	*Chaetoceros sp.*	+	-	+	1.11 ± 0.03	23	0.71 ± 0.004	9
[Mediophyceae]		+	-	-	0.52 ± 0.02	21	0.67 ± 0.02	10
		+	+	+	1.04 ± 0.06	7	0.71 ± 0.005	6
		+	+	-	0.71 ± 0.1	6	0.68 ± 0.004	4
	Skeletonema sp.	-	-	+	0.85 ± 0.06	10	0.65 ± 0.01	6
		-	-	-	0.27 ± 0.04	7	0.64 ± 0.02	5
		-	+	+	0.90 ± 0.08	4	0.66 ± 0.02	4
		-	+	-	ng		ng	
	Thalassiosira sp.	na	-	+	0.50 ± 0.02	14	0.64 ± 0.01	7
			-	-	ng		ng	
			+	+	0.40 ± 0.08	3	0.62 ± 0.05	3
			+	-	ng		ng	

Table 1.2: Growth Rates and Photosynthetic Efficiencies. Steady-state growth rates (d^{-1}) and photosynthetic efficiencies (F_v/F_m) for six cultured diatom species under vitamin B_{12} replete (+) or absent (-) conditions either treated with antibiotics (AT) (+) or not (-). The presence of a MetE gene as derived from genomic (*F. cylindrus*) or transcriptomic (all other species) sequence data is denoted by (+). Transcriptomic data is not available for *Thalassiosira* sp. (UNC1203). n denotes the number of replicate measurements. ng; no steady state growth, na; not available. ([a]) The presence of MetE was determined from genomic data in the case of *F. cylindrus*; for all other -cultured species its presence was determined from transcriptomic data where provided.

Significant differences in F_v/F_m were observed between $+B_{12}$ and $-B_{12}$ *Chaetoceros* sp. UNC1202 cultures (Mann-Whitney U Statistic = 3.5). Analysis of steady state photosynthetic efficiencies for $-B_{12}$ *P. granii* and $-B_{12}$ *Thalassiosira* sp. UNC1203 were not possible due to cessation of growth. However, F_v/F_m measurements taken before growth cessation showed a decrease in photosynthetic efficiency for both treatments prior to vitamin B_{12} addback and a corresponding increase in F_v/F_m post B_{12} addback (K.A. Ellis unpubl.). There were no significant differences in photosynthetic efficiency among treatments for the other examined diatom species.

B_{12} Addback Experiments

The results of B_{12} addback experiments indicated that while growth of *P. granii* was affected by the absence of vitamin B_{12}, *F. cylindrus* growth was not (Figure 1.1).

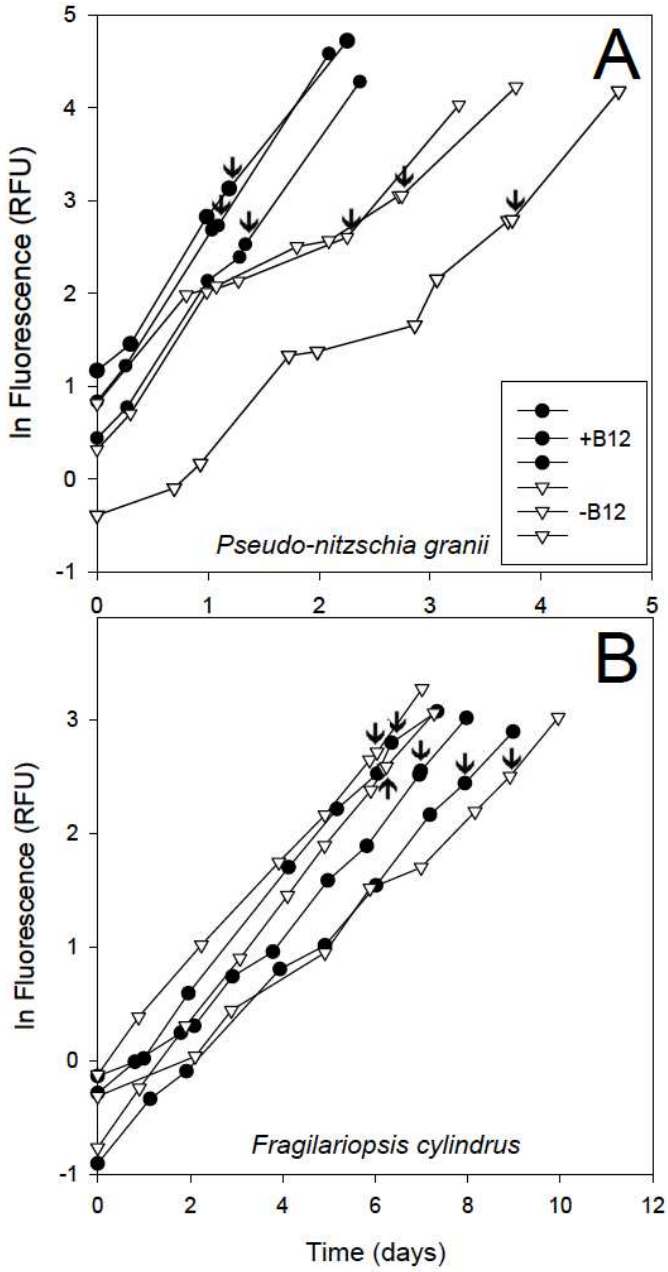

Figure 1.1. Natural log of relative fluorescence units over time for A) *P. granii* and B) *F. cylindrus* B_{12} addback experiments. Cultures were initially grown with (+B_{12}) and without (-B_{12}) vitamin B_{12}. Arrows indicate time of B_{12} addback and shape indicates B_{12} status.

The three -B_{12} replicates of *F. cylindrus* grew exponentially throughout all experiments, both before and after an addback of vitamin B_{12}. In contrast, *P. granii* grown in cultures without

vitamin B_{12} had inconsistent and reduced growth rates compared to $+B_{12}$ treatments. The growth of these cultures responded positively to the vitamin B_{12} addback. Both + and – B_{12} treatments for *F. cylindrus* had similar and consistent growth rates. No detectable growth responses to the B_{12} addback were observed in either *F. cylindrus* treatment.

While photosynthetic efficiencies differed significantly between $+B_{12}$ and $-B_{12}$ treatments pre-B_{12} addback for *P. granii* cells ($p = 0.03$), there were no similar differences for *F. cylindrus* (Figure 1.2). There were no significant differences in photosynthetic efficiencies between pre and post B_{12} addback within a treatment ($+B_{12}$ or $-B_{12}$) for either species.

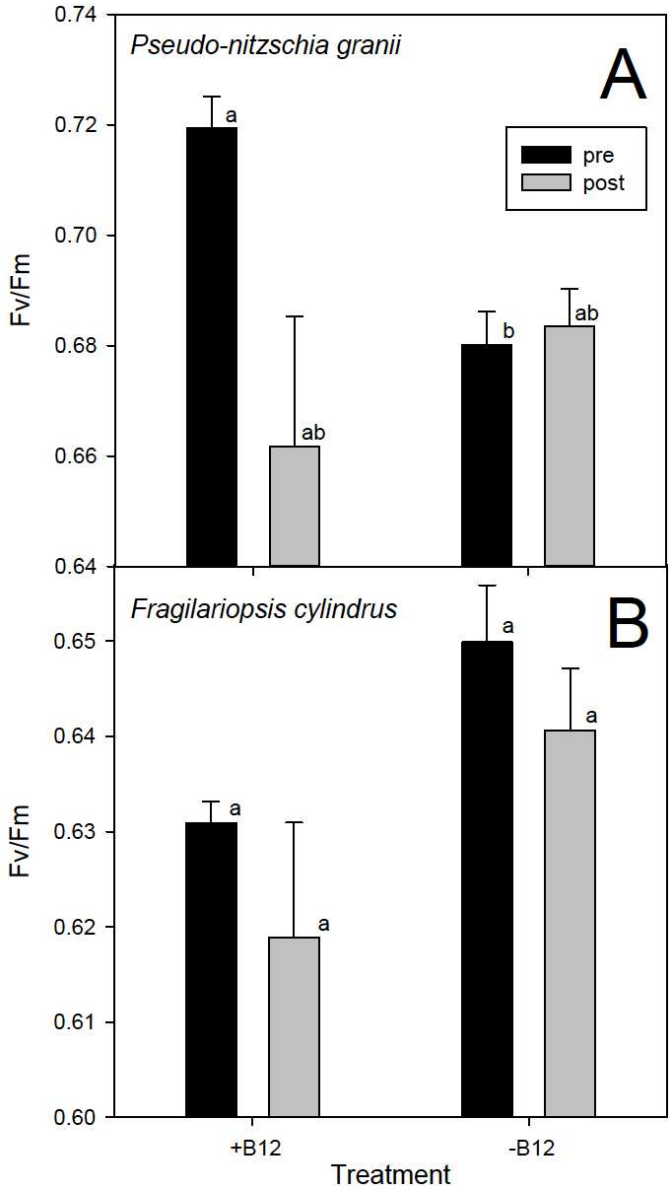

Figure 1.2. Photosynthetic efficiency (F_v/F_m) comparisons pre and post addback of B_{12} to A) *P. granii* and B) *F. cylindrus* cultures grown with (+B_{12}) and without (-B_{12}) vitamin B_{12}. Error bars represent ±1 standard error associated with the mean (n=3). Letters indicate statistically different groupings ($p<0.05$).

Gene Expression Analysis

Gene expression analysis of *P. granii* determined that the average ratio of MetH/ACT transcript copies ranged from 0.047±0.01 for $-B_{12}$ post addback to 0.17 ± 0.03 for $-B_{12}$ pre addback (Figure 1.3). Ratios of MetH/ACT in $+B_{12}$ experiments had similar variability to $-B_{12}$ pre and post addback, ranging from 0.002±0.003 to 0.15±0.02. There was no significant difference in MetH/ACT before and after B_{12} addback in $+B_{12}$ experiments, and no significant change in relative expression (Figure 1.3).

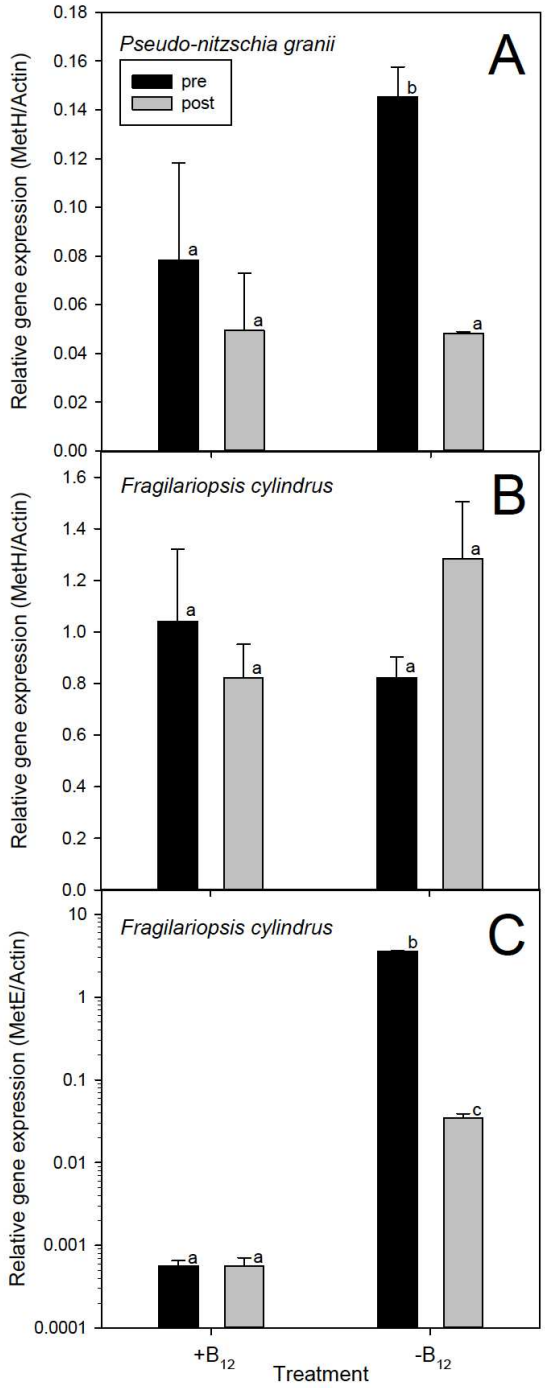

Figure 1.3. Relative gene expression of A) *P.granii* MetH, B) *F. cylindrus* MetH and C) *F. cylindrus* MetE pre and post addback of B_{12} initially grown with ($+B_{12}$) and without ($-B_{12}$) vitamin B_{12}. All genes are normalized to Actin (ACT) transcripts. MetE gene expression is on a log scale. Error bars represent ±1 standard error associated with the mean ($n \geq 3$). Letters indicate statistically different groupings ($p<0.05$)

There was a significant difference in *P. granii* MetH/ACT expression from pre to post B_{12} addback for the $-B_{12}$ treatment ($p = 0.02$), with MetH being up-regulated 3.02 fold under $-B_{12}$ conditions (Figure 1.4).

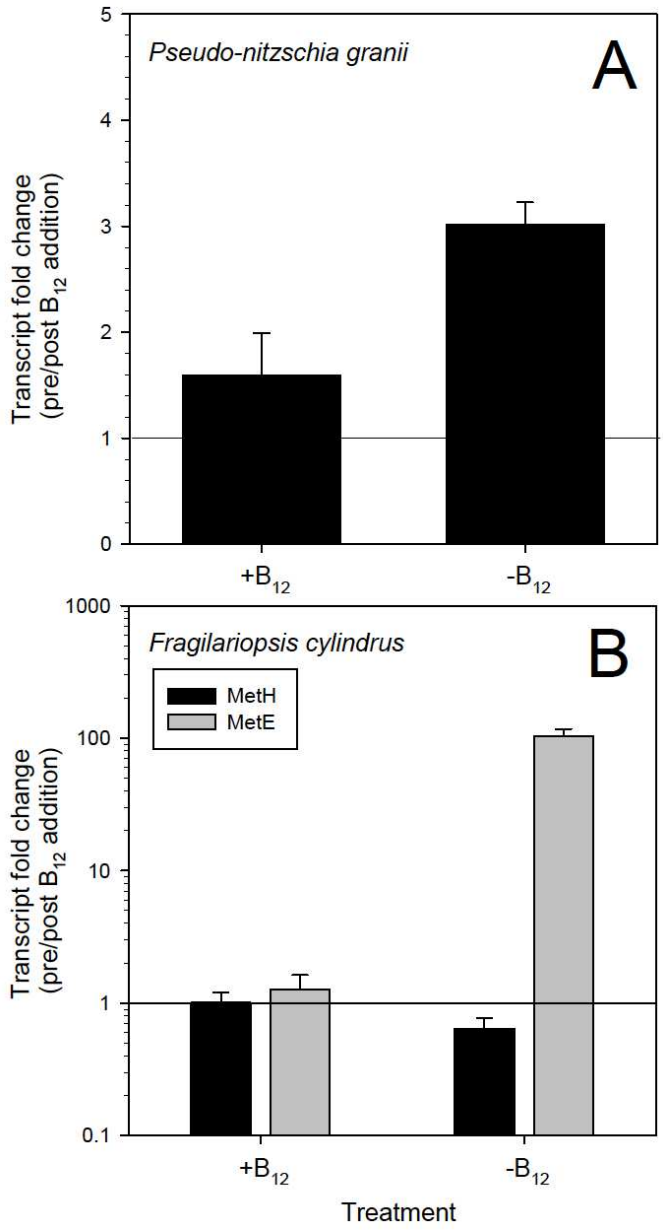

Figure 1.4. Transcript fold change in relative gene expression of A) *P. granii* MetH and B) *F. cylindrus* MetH and MetE from pre to post B_{12} addbacks. All genes are normalized to Actin (ACT) transcripts. Error bars represent ±1 standard error associated with the mean (n ≥3). Note log scale in B.

Average expression of MetH/ACT for *F. cylindrus* was constitutive across all treatments, varying from 0.61±0.02 in $-B_{12}$ pre addback to 1.5±0.05 in $+B_{12}$ pre addback (Figure 1.3). There were no significant differences in MetH/ACT expression from pre to post addback in either treatment. While there was no change in relative expression of MetH from pre to post B_{12} addback in $+B_{12}$ experiments, a fold change of 0.64 in $-B_{12}$ experiments infers that MetH was slightly up-regulated (1.5-fold) following B_{12} addition to B_{12} deficient cells (Figure 1.4).

There was no significant difference between MetE/ACT expression from pre to post addback in $+B_{12}$ experiments, while there was a significant difference from pre to post addback in $-B_{12}$ treatments ($p = 0.001$) (Figure 1.3). The relative expression of MetE in *F.cylindrus* was 103-fold greater under B_{12}-deficient conditions (Figure 1.4). MetE/ACT average transcript ratios ranged from 0.0004±0.0002 in $+B_{12}$ post addback to 3.7±0.02 in $-B_{12}$ pre addback.

Phylogenetic Tree Analysis

The MetH phylogenetic tree showed a strong grouping of many of the raphid pennates, or Bacillariophyceae, into a monophyletic clade (Figure 1.5).

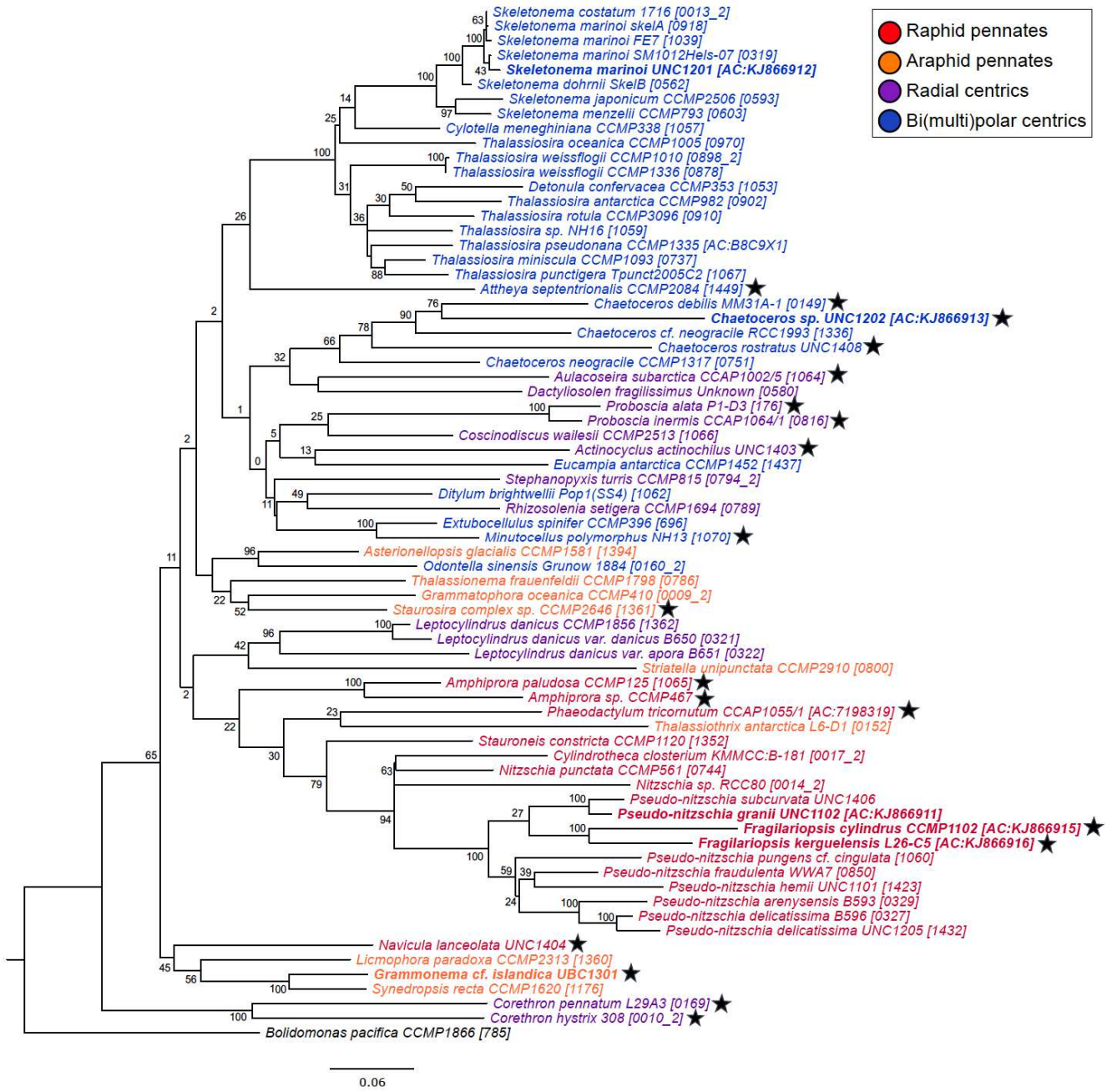

Figure 1.5. Diatom MetH sequence phylogenetic tree showing the relationship between MetH and possession of a MetE gene as indicated with a star by the diatom name. Diatom species cultured in this study are in bold. A MetH sequence for *Thalassiosira* sp. UNC1203 used in this study are not available. Font colors correspond to diatom class as described in Medlin and Kaczmarksa (2004): Raphid pennates (Bacillariophyceae) (red), araphid penates (orange), bi(multi)polar centrics (Mediophyceae) (blue), and radial centrics (Coscinodiscophyceae) (purple) Node labels show percent consensus support for tree arrangement and branch length

represents the amount of divergence between nodes (substitutions/site). *Bolidimonas pacifica* was used as the outgroup.

Although there were no consistent groupings with the other diatom classes, including araphid pennates, bi(multi)polar centrics, (Mediophyceae), and radial centrics (Coscinodiscophyceae), centrics and pennates generally formed distinct clades. Patterns in MetH sequence phylogeny were somewhat consistent with those achieved by 18S rRNA phylogeny (Medlin and Kaczmarska 2004). A full or partial sequence for MetE was identified in 22 of the 91 diatoms with whole genome or transcriptome sequences queried in this study. The presence of MetE within diatoms did not display any phylogenetic relatedness based on current available sequence data.

The MetE phylogenetic tree showed a strong grouping among the diatoms (within Heterokontphyta) and Rhizaria, but less so among other represented protist groups (Figure 1.6A). The MetE biogeography map shows a potential correlation between HNLC areas, particularly the Southern Ocean, and the possession of a MetE gene (Figure 1.6B).

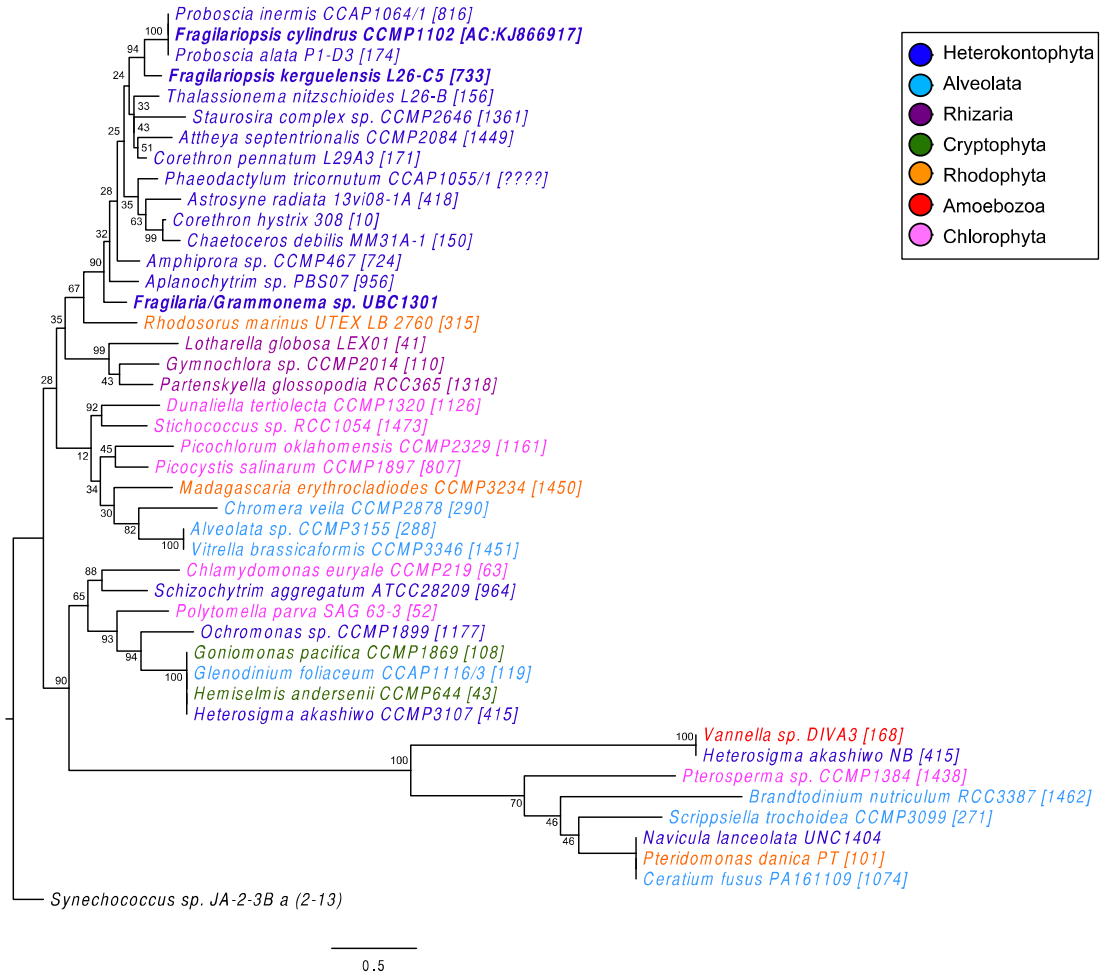

Figure 1.6. Eukaryotic protist MetE sequence phylogenetic tree showing evolutionary grouping of the MetE gene. Diatom species cultured in this study (Chapter 1 and Chapter 2) are in bold. Font colors correspond to groupings according to Parfrey et al. 2010 and Dorrell and Smith 2011. Node labels show percent consensus support for tree arrangement. Branch length represents the amount of divergence between nodes (substitutions/site). *Synechococcus sp.* was used as the outgroup.

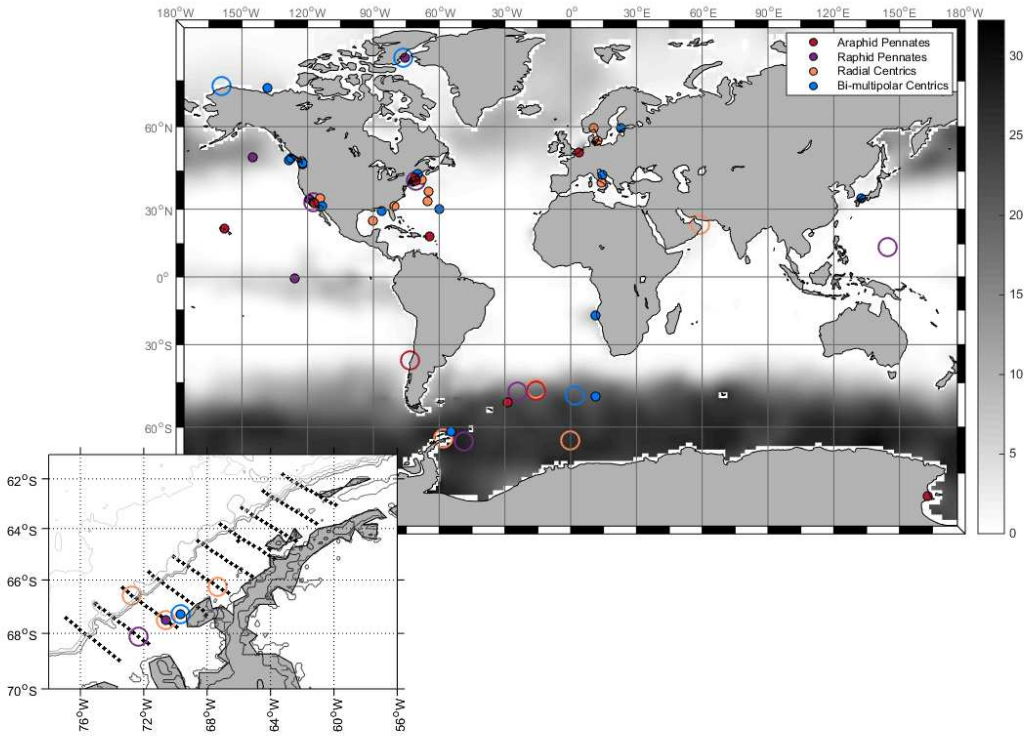

Figure 1.6B. The distribution of diatom species possessing MetE according to current genomic and transcriptomic data. Open circles represent species with MetE, while filled circles represent species with no confirmed MetE gene. Sea-surface nitrate concentrations are denoted in grayscale, with darker areas corresponding to high nutrient, low chlorophyll (HNLC) areas that are generally Fe-limited. [Credit C. Moreno, unpubl.]

Discussion

Though *Pseudo-nitzschia* and *Fragilariopsis* are closely related diatom genera (Lundholm et al. 2011), this study has demonstrated that a fundamental difference in their gene repertoires determines whether particular species from these genera are auxotrophic for vitamin B_{12}. Variations in nutrient requirements among organisms can lead to different responses to changing environmental conditions. These responses can in turn influence community dynamics

and succession when the nutrient, such as vitamin B_{12}, is required for one species but not for another.

In 3 of 4 diatom species cultured in this study, the absence of a MetE gene (based on our initial screens of available sequence information) correlated with no growth in the absence of vitamin B_{12}. In the case of the B_{12}-auxotrophic *P. granii*, growth without B_{12} resulted in significant up-regulation of the MetH gene. This MetH up-regulation was not observed in *F. cylindrus*, however, indicating that *P. granii* may compensate for a methionine deficit through increased MetH expression as seen in previous studies (Bertrand et al. 2012). *Thalassiosira* sp. UNC1203 and *Skeletonema* sp. UNC1201 both ceased growth in AT $-B_{12}$ cultures, similar to *P.granii*. However, the severity of the B_{12} deprivation response differed between species in non-AT medium. While *Skeletonema* sp. continued growth in non-AT $-B_{12}$ medium, albeit at reduced rates, *P. granii* and *Thalassiosira* sp. could not grow without B_{12} additions even in the presence of bacteria. Similarly, the *Chaetoceros* sp. UNC1202 examined in this study grew at reduced rates without vitamin B_{12} despite evidence of MetE in its gene repertoire. These trends occurred regardless of whether bacteria were present or substantially reduced after antibiotic treatment, suggesting the bacterial communities present in the medium were not providing a significant supply of B_{12} to these diatoms. Thus, varying responses to B_{12}-limitation are more likely a consequence of differences in internal B_{12} quotas and B_{12} uptake rates as well as the presence or absence of MetE.

The appreciable decrease in growth rates of *Chaetoceros* sp. in $-B_{12}$ medium despite the presence of MetE could be due to the relative catalytic inefficiency of MetE compared to MetH, supported by the results of gene expression analysis in this study, which found that MetE was

up-regulated far beyond levels of MetH when used. This implies many more MetE enzymes are needed to produce the methionine of one MetH enzyme (Banerjee and Matthews 1990). This inefficiency may not adversely affect organisms in polar regions where slow-growing diatoms such as *F. cylindrus* and *F. kerguelensis*, the other two MetE-possessing diatoms in this study, are primarily found. However the *Chaetoceros* sp. UNC1202 had a much higher maximum growth rate than that of the *Fragilariopsis* species. The lower maximum rate of MetE catalyzation, therefore, could limit *Chaetoceros* sp. UNC1202 growth rates but be sufficient for *Fragilariopsis* species to maintain similar growth rates regardless of B_{12} supply (O'Brien et al. 2013). Lastly, *Chaetoceros* sp. UNC1202 could have a higher B_{12} quota than the other species examined in this study because of variations in less-studied pathways, such as the B_{12}-requiring methylmalonyl-CoA mutase enzymatic pathway (Helliwell et al. 2011).

Although it was not possible to determine steady-state photosynthetic efficiencies for cultures that ceased growth in the absence of B_{12}, variations in photosynthetic efficiencies were observed among other diatom species. For *Chaetoceros* sp. UNC1202 in particular, F_v/F_m decreased in cultures when B_{12} was absent from the medium. Vitamin B_{12} may affect photosynthetic processes downstream—phylloquinone (vitamin K) is a hypothesized electron carrier in photosystem I and requires S-adenosyl methionine, which is B_{12}-dependent, for its creation (Lohmann et al. 2006). In this case, as was seen within our *P. granii* addback cultures, growth cessation was most likely responsible for the lowered F_v/F_m values. Alternatively, diatom species could be shifting the dominant electron transfer mechanism in photosystem I from vitamin K to Fe under B_{12}-limited conditions (King et al. 2011). B_{12} has also been shown to exert control over bacteriochlorophyll production in some bacteria, although its role within diatoms has yet to be elucidated (Cheng et al. 2014).

As demonstrated by this study, vitamin B_{12} auxotrophy is not confined to pennate or centric diatoms but is instead distributed irrespective of phylogeny across genera. Although *P. granii*, *F. cylindrus*, and *F. kerguelensis* are raphid pennate and *Thalassiosira* sp., *Chaetoceros* sp., and *Skeletonema* sp. are bi(multi)polar centric diatoms, B_{12} auxotrophy was found in the pennate *P. granii*, the centric *Thalassiosira* sp., and the centric *Skeletonema* sp. This study's phylogenetic analysis of diatom MetH sequences supports other broader analyses of B_{12} limitation in algal groups (Helliwell et al. 2011) by demonstrating a seemingly scattered presence of MetE within a MetH-based tree that is, for the most part, phylogenetically conserved. Some diatom genera within the tree show either complete MetE absence (e.g. *Skeletonema*) or presence (e.g. *Fragilariopsis*). However, within other genera, such as *Chaetoceros* and *Corethron*, some species possess MetE while others seem to not, based on currently available sequence information. As a larger number of diatom genomes and transcriptomes are sequenced, the prevalence of this species-specific MetE possession will be made clearer, but these initial findings suggest that MetE presence/absence is possibly species-specific.

Our results support the hypothesis that diatom species without MetE became auxotrophic for B_{12} through multiple independent losses of MetE, possibly because they resided in environments with high B_{12} concentrations (Helliwell et al. 2011). Perhaps this concept can help provide insights as to whether B_{12} is present at limiting concentrations in large areas of the ocean—if over half of surveyed algal species are auxotrophic for the nutrient, this may imply adequate concentrations of B_{12} in large areas of the ocean, either now or in the past (Croft et al. 2005).

The extreme down-regulation of MetE expression in the presence of vitamin B_{12} seen in this study provides a mechanism for loss of the gene. Because of the increase in nitrogen and

zinc requirements by the MetE enzyme and its catalytic inefficiency, MetE expression is likely repressed except when B_{12} is absent to make the most energetically efficient use of nutrients (Bertrand et al. 2013). When a down-regulated gene is used only episodically, such as in the case of MetE, mutations to the gene under B_{12}-replete conditions would not be strongly selected against, possibly leading to the development of auxotrophic algal species. The MetE tree created in this study is consistent with the theory of MetE acquisition early in diatom evolution, with subsequent losses of the gene as environmental conditions selected against it.

Because of this, our study demonstrates that in the case of vitamin B_{12} requirements, phylogeny does not predict ecology. Though diatoms such as *F. cylindrus* and *P. granii* are closely related, the difference in the presence of an isoform of a single gene can result in the survival of one species and the death of the other. As a consequence, phylogenetic relationships between diatoms are not a good predictor of which species will succeed in areas of the ocean where vitamin B_{12} availability has been shown to be potentially limiting.

Though transcriptomic information for a larger sample of diatoms is needed to fully analyze whether this MetE phylogeny is biogeographically based, the MetE distribution map indicates that many HNLC species, particularly those in polar regions, possess the MetE gene while coastal species do not. Sanudo-Wilhelmy et al. (2012) found that differences in B_{12} concentrations off the coast of California were associated with water mass origin, meaning that it is likely that abiotic factors such as water temperature are playing a role in B_{12} distribution. The success of auxotrophic diatoms is linked to the presence of B_{12} –producing bacteria, and polar diatoms could be more likely to possess MetE because slower bacterial metabolic rates in colder climates lead to lower B_{12} production rates (Church et al. 2000, Kirchman et al. 2009). Lower

densities of bacteria and cyanobacteria have also been observed in polar regions (Boyd et al. 2000).

As bacteria and archaea are the ultimate sources of vitamin B_{12}, their presence or absence undoubtedly affects the distribution and concentration of B_{12} in marine environments. Recent studies have argued that bacterial abundances could influence the response of phytoplankton communities to Fe and B_{12} additions where B_{12} becomes limiting after the alleviation of Fe limitation (Bertrand et al. 2007). However, in light of our results, bacterial abundances alone are likely not sufficient to explain the dynamics of B_{12} limitation. We propose instead that variations in B_{12} requirements among diatom (and other phytoplankton) species could explain the observed differences in diatom assemblages following B_{12} and Fe enrichment in HNLC regions.

In the aforementioned study (Bertrand and Saito 2007) a series of three B_{12}/Fe fertilization experiments performed with natural algal assemblages found that the two incubations where B_{12}/Fe additions resulted in higher phytoplankton biomass than Fe alone were dominated by *Pseudo-nitzschia subcurvata*, which interestingly has a 98.9% similar Internal Transcribed Spacer 1 (ITS1) sequence to *P. granii* (Marchetti et al. 2008) and has been verified to lack MetE through transcriptomic analysis (Moreno, unpubl). As ITS1 sequences are often used for species identification, this suggests *P. subcurvata* and *P. granii* are very closely related and are possibly subspecies. The third incubation which exhibited no further increases in phytoplankton biomass after addition of vitamin B_{12} and Fe versus Fe alone was dominated by *Fragilariopsis cylindrus*. As our study shows, all examined *Pseudo-nitzschia* species require vitamin B_{12} because it lacks the MetE isoform of methionine synthase, while *Fragilariopsis cylindrus* grows equally well with or without B_{12} due to its possession of the MetE gene. The results of our study suggest that the growth response patterns observed in Bertrand et al. (2007)

are likely affected by the diatom composition as much as they are by variations in bacterial abundances among the experiments.

Vitamin B_{12} is one nutrient among many, but its potential to be limiting or co-limiting during nutrient enrichments highlights its important role in diatom bloom dynamics. King et al. (2011) stated that under environmental conditions with low B_{12} concentrations, primary productivity can be limited by this nutrient. Our study shows that while B_{12} may limit primary production of a particular diatom species, primary production across the diatom community as a whole may be unaffected as B_{12} auxotrophs are supplanted by diatoms possessing MetE. Although bacterial abundances and composition undoubtedly help to determine B_{12} concentrations, the B_{12} requirements of the phytoplankton themselves direct how assemblages respond to those concentrations.

As shown here, molecular-level differences between diatom species such as *Pseudo-nitzschia* and *Fragilariopsis* can have ecological consequences. A recent study demonstrated a taxonomic shift from *Pseudo-nitzschia* sp. to *Fragilariopsis* sp. under Fe-replete, high CO_2 conditions in the Weddell Sea, Antarctica, suggesting species-specific differences in inorganic carbon acquisition (Hoppe et al. 2013). Similarly, the physiological responses of *P. granii* and *F. cylindrus* to the absence of vitamin B_{12} corresponded to differences in their respective gene repertoires. The composition of diatom assemblages in areas where Fe concentrations are limiting and B_{12} concentrations are low will determine how those assemblages respond to inputs of Fe. *Fragilariopsis* sp. and *Pseudo-nitzschia* sp. are ecologically important diatom genera and can be found coexisting in the same regions of the ocean. However, *Fragilariopsis* sp. are more heavily silicified compared to *Pseudo-nitzschia* sp. (Baines et al. 2010) and therefore export less carbon per silicon. Thus, under post-Fe enrichment B_{12}-limited conditions, *Fragilariopsis*-

dominated blooms could equate to greater silicon sequestration relative to carbon when compared to blooms dominated by *Pseudo-nitzschia*, affecting the diatom-derived carbon sequestration potential throughout the ocean (Assmy et al. 2013). In this light, variations in B_{12} concentrations could have far-reaching effects on the biological carbon pump not only in present oceans but also those of the past and future.

CHAPTER 2: THE COEFFECTS OF IRON AND VITAMIN B_{12} ON THE DYNAMICS OF MARINE IRON FERTILIZATION EVENTS

Introduction

Iron

Iron exists as a variety of chemical species in the marine environment, including inorganic soluble and inorganic insoluble species, dissolved organic complexes, mineral particles, colloids, and within living cells. The distribution of dissolved Fe is continually changed by the formation of colloidal particles, followed by aggregation into larger particles that sink out of the euphotic zone and thus become lost to phytoplankton use (Moore and Braucher 2008).

At the cellular level, the ability of Fe to exist in different oxidation states means that it is often used as a component of redox reactions within the cell. Iron is particularly important for phytoplankton because of its catalytic role in photosynthesis and respiratory electron transport. It is a crucial part of the cell's photosynthetic apparatus, particularly photosystems I and II as well as the cytochrome b_6f complex, and is found in higher proportions there under Fe limitation (Raven 1988, Greene et al. 1991).

Although Fe exists in many forms, contemporary Fe concentrations in the ocean are low—generally in the picomolar to nanomolar range, and at such scarcity in HNLC regions that phytoplankton growth is limited by it (Wells et al. 1995). The oxidized ferric (Fe(III)) Fe species is the most stable in seawater, with most Fe(III) existing as dissolved hydrolysis species and a minority as free hydrated Fe(III) ions (Rue and Bruland 1995). It is thought that inorganic Fe species are the main means by which phytoplankton obtain Fe, in addition to colloidal Fe that

has been transformed by thermal, photochemical, or biological reduction (Hutchins 1995). In addition, the majority of dissolved Fe is bound to organic ligands and bacteria-synthesized compounds called siderophores. Iron bound in this way is kept from oxidizing to Fe(III), but is also difficult for phytoplankton to access (Rue and Bruland 1995).

The flux of Fe into the euphotic zone is highly spatially variable and dependent on a variety of sources. These sources include terrestrial run-off, wind-blown dust, precipitation, deep water upwelling, and anthropogenic inputs (Wetz et al 2006, Klunder et al 2012, Lohan and Bruland 2008, Mahowald et al 2005). In polar regions, glaciers may also be a significant source of Fe to the ocean. As icebergs are discharged from glaciers into open water and begin to melt, the continental debris (including Fe) suspended within them will be discharged into the surrounding water. Sea ice also serves as a source of Fe to high-latitude areas. The ice surface accumulates Fe-laden dust, and delivers that dust to biological communities in the water beneath as it melts (Raiswell et al. 2008). Because Fe is generally reactive and insoluble, knowing the magnitude and type of Fe flux is important in determining Fe availability to primary producers (Johnson et al 1997).

Vitamin B_{12}

Researchers have long known that most eukaryotic phytoplankton require an outside source of vitamins for use as cofactors in enzyme creation, the most ubiquitous of which are the B vitamins (Sañudo-Wilhelmy et al. 2012). One of these, vitamin B_{12}, has two important bioavailable forms: adenosylcobalamin and methylcobalamin (Raux et al. 2000). While adenosylcobalamin has an R group of 5'-deoxy-5'adenosyl ligands and is utilized as a cofactor in isomerases, methylcobalamin's R group is comprised of methyl ligands and it functions as a

cofactor in methyltransferases (Gruber et al. 2011). One isoform of methionine synthase in particular (MetH) has been shown to depend on methylcobalamin as a cofactor in order to catalyze the synthesis of the essential amino acid methionine (Banerjee 1990, Rodionov et al 2003). While some marine algae also possess an alternate form of the enzyme that does not require B_{12} (MetE), over half of algal species are estimated to only possess MetH (González et al. 1992, Croft et al. 2005). The majority of isolates examined for MetE thus far have been coastal diatoms, begging the question of whether this trend in auxotrophy holds true among oceanic and polar species. A strong correlation between the absence of a functional MetE gene and B_{12} auxotrophy has been found in a wide range of algal species (Helliwell et al. 2011).

Although vitamin B_{12} functions mostly as a cofactor for MetH in diatoms, upstream and downstream processes may also be affected when B_{12} is unavailable to auxotrophic organisms. Folate, vitamin B_{12}, and PLP (vitamin B_6) metabolisms are linked in diatoms through a complex series of reactions (Bertrand et al. 2012). Upstream of the point where methionine is synthesized, PLP synthase creates vitamin B6, which is then used along with cytosolic serine hydroxymethyltransferase (cSHMT) in the reversible conversion of serine and tetrahydrofolate (THF) to glycine and 5,10 methylene THF (Appaji et al. 2003). Tetrahydrofolate is then used in nucleic acid synthesis, while 5,10 methylene THF is irreversibly converted to 5-methyl-THF using methylene-tetrahydrofolate reductase (MTHFR) (Bertrand et al. 2012).

Methionine synthase, either in the form of the B_{12}-dependent MetH or the B_{12}-independent MetE, is then used to regenerate methionine from homocysteine while simultaneously turning 5-methyl THF into tetrahydrofolate (Matthews et al. 2003). Without the conversion of 5-methyl THF into tetrahydrofolate, methyl-THF accumulates and "folate trapping" occurs. This results in a folate deficiency that can affect processes such as DNA

synthesis (Hoffbrand and Weir 2001). Methionine regeneration is an important part of the S-adenosyl methionine (SAM) cycle, as SAM is synthesized from ATP and methionine in two consecutive reactions. The availability of S-adenosyl methionine is important in downstream processes as well, as it functions as a cosubstrate in methyl group transfers (Bertrand and Allen 2012). ThiC, a thiamine biosynthesis protein, is also SAM dependent and has been shown to respond to B_{12} limitation in algal cultures (Bertrand and Allen 2012).

Methionine and SAM are both required for DMSP production, which is used by some diatoms as a cryoprotectant, osmolyte, or antioxidant. DMSP is also the precursor to dimethylsulfide, a climatically important gas that may provide the nuclei for cloud condensation (Malin et al 1992). Antarctic diatoms in particular are known to produce relatively large amounts of DMSP, and so their metabolisms may demand more methionine synthase activity (Bertrand et al 2013). The other major enzyme that utilizes vitamin B_{12} as a cofactor is methylmalonyl-CoA mutase, which catalyzes the isomerization of methylmalonyl-CoA to succinyl-CoA and is used in fatty acid metabolism (Bertrand et al 2012).

The sole source of vitamin B_{12} to marine organisms is heterotrophic bacteria, archaea, and cyanobacteria, which synthesize this vitamin through a complicated series of over 20 enzymatic reactions. Eukaryotic phytoplankton must therefore obtain all their vitamin B_{12} from bacterial sources, whether through symbiotic interactions or scavenging after cell lysis (Croft et al 2005, Droop 2007).

The distribution of vitamin B_{12} in the ocean is potentially affected by variations in cobalt concentrations, as cobalt is an integral part of vitamin B_{12}; it is the central cation held by a corrin ring within the B_{12} molecule. Panzeca et al (2008) and Bonnet et al (2013) found that abundances of B_{12} and cobalt were correlated, with higher cobalt concentrations found alongside higher

concentrations of B_{12}. Cobalt distribution is very likely related to aeolian and riverine sources, meaning that coastal areas are likely to have higher and more sustained cobalt concentrations. This could be a partial explanation for why higher concentrations of vitamin B_{12} are generally seen in coastal areas (Panzeca et al 2009).

Vitamin B_{12} concentrations in the ocean are in the picomolar range, and vary widely depending on the environment (Koch et al 2011, Bonnet et al 2013, Panzeca et al 2009). B_{12} concentrations generally increase poleward and at intermediate depths (Sañudo-Wilhelmy et al 2012). It seems probable that sustained upwelling conditions may contribute to higher B_{12} concentrations at the ocean's surface (Panzeca et al 2009, Bonnet et al 2013). Koch et al (2011) found that vitamin B_{12} concentrations were four times higher in HNLC regions as compared to off-shelf and coastal regions, although opposite trends have been observed in other studies (Sañudo-Wilhelmy et al 2014). Incubation experiments showed that vitamin B_{12}, alone or in conjunction with other primary limiting nutrients such as Fe or nitrate, was able to significantly increase phytoplankton growth rates and influence phytoplankton composition (Koch et al 2011).

Iron and Vitamin B_{12} Interactions

Although cobalt is the primary trace metal utilized in vitamin B_{12} synthesis, there is the potential for interactions between Fe and B_{12} availability in marine systems. Bacterial vitamin B_{12} uptake may increase under iron limitation because of its use in ribonucleotide reductase—an enzyme that can use either Fe or vitamin B_{12}, but which is thought to utilize B_{12} only when Fe is not available (Borovok et al 2006). This means that an Fe fertilization event could result in an increase in B_{12} availability to phytoplankton by decreasing bacterial demand and increasing bacterial abundances, as bacteria also require Fe to grow (Bertrand et al 2013). Subsequent Fe-

B_{12} interactions in diatoms could be the result of a change in species composition, an increase in vitamin transporters, or an increase in the energy allocated to vitamin transport systems to keep vitamin uptake rates in line with growth rates (Bertrand et al 2011).

Colimitation of vitamin B_{12} and Fe has been observed on a large scale in areas such as the Southern Ocean (Bertrand and Saito 2007). While B_{12} alone was not limiting to phytoplankton growth, Fe and B_{12} additions together increased growth over that of Fe alone. Even when B_{12} additions do not change rates of primary production, increases in its concentration can alter phytoplankton community composition, enhancing the abundances of primarily B_{12}-auxotrophic groups. Although many diatoms are auxotrophic for B_{12}, fertilization experiments in the Gulf of Alaska found that flagellates outcompete diatoms after B_{12} addition, creating a phytoplankton community less likely to export carbon than the diatom-dominated communities found after Fe fertilization (Koch et al 2011). However, the addition of both Fe and B_{12} has the potential to alter these community dynamics even further.

On a cellular level, the C:P and N:P ratios of B_{12}-limited diatoms are significantly lower in comparison with B_{12}-replete cells, particularly at high CO_2 concentrations (King et al 2011). Fe-limited diatoms also show lower cellular levels of carbon, nitrogen, and phosphorus (Takeda et al 1998). In addition, cells grown under B_{12}-replete, high CO_2 conditions had lower Fe quotas than those grown under low CO_2 (King et al 2011). However, another study found no large growth rate differences between *Phaeodactylum tricornutum*, which possesses MetE, and *Thalassiosira pseudonana*, which does not, when grown under varying Fe and B_{12} conditions. Neither diatom showed a significant difference in growth rate between low Fe and low Fe/low B_{12} treatments (Bertrand et al 2012).

Vitamin B_{12} can affect photosynthetic processes downstream from methionine synthase. Phylloquinone (vitamin K) is an electron carrier in photosystem I and requires S-adenosyl methionine, which is B_{12}-dependent, for its creation (Lohmann et al. 2006). It has previously been suggested that B_{12} limitation could limit phylloquinone production and impair photosynthesis, but this effect was only observed physiologically when Fe, another electron carrier, was unavailable (King et al. 2011).

Although vitamin B_{12} and Fe are not among the classical nutrients required for phytoplankton growth (namely nitrogen and phosphorus), availability of these micronutrients may interactively affect macronutrient requirements and availability. Creation of MetE requires in a 30-fold increase in nitrogen and 40-fold increase in zinc allocated to methionine synthase activity relative to MetH usage (Bertrand et al 2013). More broadly, Fe is required for the reduction of nitrate to ammonium, both in Fe-containing reductases and the photosynthetic processes that provide energy for the reaction (Takeda et al 1998). In turn, nitrate is utilized in B_{12} molecules themselves, as well as in enzymes such as methionine synthase that are involved in B_{12}-dependent processes (Banerjee and Ragsdale 2003). Under Fe limitation, diatoms reduce uptake of nitrate and it has been suggested that nitrogen starvation could upregulate pathways that require B_{12}, such as methionine and SAM synthesis (Bertrand and Allen 2012).

Iron and B_{12} cycling are complicated even when viewed in isolation, with biotic and abiotic components mediated by species-specific interactions between microbial groups. To obtain a more accurate view of what is occurring in marine environments, we must attempt to examine how these nutrients interact with one another. We know that Fe and B_{12} can be colimiting, and that they can react synergistically with one another to increase phytoplankton growth beyond what either could do alone. Examining these processes at the cellular and

molecular level will allow us to better understand the potential for large scale variations in carbon or silica sequestration, nutrient cycling, and phytoplankton community succession and composition in HNLC areas.

In this study, we will compare the responses of diatom species to varying Fe and vitamin B_{12} availabilities using physiological and molecular techniques. We will grow antibiotic-treated *P. granii* and *G. cf. islandica* in a Fe/B_{12} culture matrix and examine growth rates, photosynthetic efficiencies, gene expression, and chl *a* contents per cell. We hypothesize that B_{12}-auxotrophic diatoms, such as *P. granii*, will have a greater response to Fe/B_{12} colimitation than limitation of either nutrient alone because of the potential for upstream and downstream processes to be affected. Diatoms with MetE may be stressed further by Fe/B_{12} colimitation because of a combination of MetE's higher nitrate requirement and decreased nitrate reductase rates as a result of Fe limitation.

Methods

Algal species

Isolates of two diatom species were examined during this study (Table 1.1). *Pseudo-nitzschia granii* (UNC1102) (G.R. Hasle) was obtained from Ocean Station Papa (50°00 N, 145°00 W) in the Northeast Pacific Ocean in 2010 (18S Genbank accession number KJ866907) and *Grammonema cf. islandica* (UBC1301) was also obtained from Ocean Station Papa in 2013. *Grammonema cf. islandica* was identified based on a 99% homology to an 18S rDNA (ribosomal deoxyribonucleic acid) sequence deposited in Genbank (accession number AJ535190). Genbank accession numbers for MetH are indicated in Figure 1.5, while those for MetE are listed in Appendix 2.

Medium and culture conditions

All phytoplankton cultures were grown in artificial seawater medium [Aquil] using trace metal clean [TMC] techniques as according to Marchetti et al. (2006). Macronutrients were added to Aquil medium in final concentrations of 300 μmol L^{-1} NO_{3-}, 10 μmol L^{-1} PO_{3-}, and 100 μmol L^{-1} $Si(OH)_4$ to achieve macronutrient-replete growth. All dispensing of medium occurred under a positive-pressure, laminar-flow hood. Before use, Aquil medium was microwaved in a 2-L Teflon bottle for sterilization. Medium was dispensed into 2-L acid-cleaned, milli-Q H_2O-rinsed polycarbonate bottles and supplemented with filter-sterilized (0.2-μm Acrodisc) Fe, ethylenediamine tetraacetic acid [EDTA] trace metals, and vitamins (thiamine and biotin) according to Aquil medium concentrations (Price et al. 1988/89). Pre-filtered vitamin B_{12} was added so that its concentration in the medium was $5.5 \cdot 10^{-7}$ kg m^{-3} (405 pmol L^{-1}) for a B_{12}-replete treatment [$+B_{12}$], or was excluded altogether to create B_{12}-absent medium [$-B_{12}$]. Trace-metal concentrations were buffered using 100 μmol L^{-1} of EDTA. Premixed Fe-EDTA (1:1) was added at total concentrations of 1.37 μmol L^{-1} to achieve free ferric-ion concentrations of 10^{-19} mol L^{-1} [pFe 19], which was considered to be Fe-replete medium [+Fe]. For *P. granii*, Fe-limited medium [-Fe] was created by adding premixed Fe-EDTA (1:1) at total concentrations of 1.55 nmol L^{-1} to 50 μL of 200 nM deferoxamine [DFB]. The Fe:DFB solution was allowed to equilibrate overnight before being added to 1 L of medium. For *Grammonema cf. islandica* Fe limitation was achieved by adding premixed Fe-EDTA (1:1) at total concentrations of 8.59 nmol L^{-1} to achieve free ferric-ion concentrations of $10^{-21.2}$ mol L^{-1} [pFe 21.2]. The Aquil medium was allowed to chemically equilibrate overnight before use and was stored in a TMC room.

For steady-state culturing conditions, refer to the "Medium and culture conditions" section of Chapter 1 of this thesis.

Iron Addback Experiments

Changes in growth and gene expression in response to vitamin B_{12} and Fe co-limitation, as well as short-term response to Fe addition, were measured for *P. granii* and *Grammonema cf. islandica* by growing cultures under AT +/- B_{12}/Fe conditions (+B_{12}/+Fe, -B_{12}/+Fe, +B_{12}/-Fe, -B_{12}/-Fe) and performing an addback of Fe to the growth medium. These species were chosen because, in addition to being isolated from the HNLC North Pacific, one (*P. granii*) is auxotrophic for B_{12} while the other (*G. cf. islandica*) possesses MetE. Cultures were grown under similar conditions as described above in modified TMC, 2-L polycarbonate bottles with Teflon tubing to permit subsampling while minimizing contamination. All subsampling was performed under a positive-pressure, laminar-flow hood. A Teflon stir bar was added to each experiment and was incubated on top of a stir plate to ensure the culture remained well mixed. Aquil medium was prepared using the same methodology as described previously and inoculated using steady-state growth cultures. All experiments were inoculated when cultures were in mid-exponential growth phase and, except in the case of B_{12}-limited *P. granii* and Fe-limited *Grammonema cf. islandica* treatments, cultures were transferred into the same treatment they were previously acclimated to.

Because *P. granii* growth ceased after approximately 2 transfers in –B_{12} medium in both non-AT and AT cultures, +B_{12} –grown *P.granii* cultures (18 mL) were used as the inoculum for the –B_{12}/+Fe or –B_{12}/-Fe treatments. A similar procedure was used to grow Fe-limited *Grammonema cf. islandica*. Steady-state cultures were transferred from pFe 21.2 medium into

lower medium containing a lower Fe concentration (total Fe concentrations of 6.24 nmol L^{-1} and free ferric Fe concentrations of $10^{-21.35}$ mol L^{-1}) to achieve Fe-limited growth. Fluorescence measurements of subsamples were taken from each culture once each day for +Fe treatments, and once every other day for –Fe treatments. F_v/F_m measurements were performed using the same methodology as described in Chapter 1. The length of experiments varied among diatom species and experimental treatments, but was typically between 5-15 days.

When fluorescence measurements indicated that cultures were in late exponential growth phase, 5-mL aliquots were subsampled for F_v/F_m and fluorescence measurements. 450 mL of each culture was then filtered onto a 3.0-µm polycarbonate filter; the filter was immediately frozen in liquid nitrogen, and stored at -80°C until RNA extraction. 50 mL was filtered onto a GF/F filter and stored at -80°C until chlorophyll *a* analysis, while 200 µL of Lugol's solution was added to 5 mL of culture to preserve cells for counts.

After the initial time point, the remainder of +Fe cultures was discarded and experiments were considered concluded. For the –Fe cultures, an Fe addition of 97.8 µL (1.37 µmol L^{-1}) was added to the remaining culture immediately following the first filtration to simulate the effects of a natural Fe enrichment event. Resultant Fe concentrations (10^{-19} mol L^{-1}) are well above those needed to achieve Fe-replete growth of the diatom cultures. Cultures were then incubated for an additional 24 hours before the same set of filtrations were repeated, with the exception of the volume filtered for RNA being reduced to 300 mL due to higher cell densities. In addition, before the final filtration of the Fe-resupplied cultures, a 2 mL subsample was collected to check for bacterial contamination using the SYBR-stain method as described in Chapter 1.

Gene expression analysis

Primers for qPCR were developed using Primer 3 and tested using PCR, gel electrophoresis, and PCR product sequencing (Appendix 1). See Chapter 1 for RNA extraction, RT-pcr, and qPCR methods.

Transcript copy numbers were normalized to Actin [ACT] copy numbers from the same cDNA sample. The Actin gene was used as a housekeeping gene for both *P. granii* and *Grammonema cf. islandica* and is a commonly-used housekeeping gene that remains stable under a variety of nutrient regimes (Alexander et al. 2012).

Chlorophyll a and Cell Count Analysis

Cell enumeration was performed for all Fe-resupply cultures, pre and post Fe addition, as well as +Fe culture using an Olympus CKX41 Inverted microscope. Cell counts were determined using a 1-mL Sedgewick-Rafter counting chamber after allowing cells to settle for 5 minutes and counting >300 cells or 30 fields of view.

Chl *a* was measured using the in vitro fluorometric technique (Parsons et al. 1984). Chl *a* concentrations on filters were determined through extraction in 5 ml of 90% acetone at -20°C for 24 hours. Each sample was then diluted 10-fold in 90% acetone and fluorescence was measured before and after acidification on a Turner Designs 10-AU fluorometer. Chl *a* concentrations were normalized by cell counts to obtain cellular chl *a* quotas in pg $cell^{-1}$.

Statistical Analyses

To test for significant differences between treatments, two-tailed homoscedastic t-tests within each species were performed on steady-state culture growth rate data. Two-tailed

homoscedastic t-tests were also performed to test for significant differences between F_v/F_m and sigma (σ_{PSII}) values between treatments. A two-tailed pairwise t-test was performed between the gene expression ratios, Fv/Fm values, and sigma values for Fe-limited and Fe-resupply values for the B_{12} addback experiments. Two-tailed homoscedastic t-tests were performed between Fe-replete treatments and Fe-limited/resupply treatments.

To reduce technical error, the standard deviation of the mean for each triplicate ratio measurement was <10% of the mean. The level of statistical significance for all tests was $p<0.05$. All tests were performed in Sigmaplot 12.5 (Systat Software Inc.) and passed the Shapiro-Wilk Normality Test and Equal Variance Test.

Results

Steady-State Growth Rates and Photosynthetic Efficiencies

Steady-state growth rates and photosynthetic efficiencies for $-B_{12}$ treatments (+Fe and –Fe) could not be obtained for *P. granii*, as cultures ceased growth after 2 transfers into B_{12}-absent medium. For *P. granii*, there was no significant difference between AT and non-AT growth rates, regardless of treatment (Figure 2.1). However, growth rate significantly decreased under Fe limitation (+B_{12}/-Fe) relative to Fe-replete conditions ($p = 4 \times 10^{-7}$ for non-AT, $p = 2 \times 10^{-4}$ for AT).

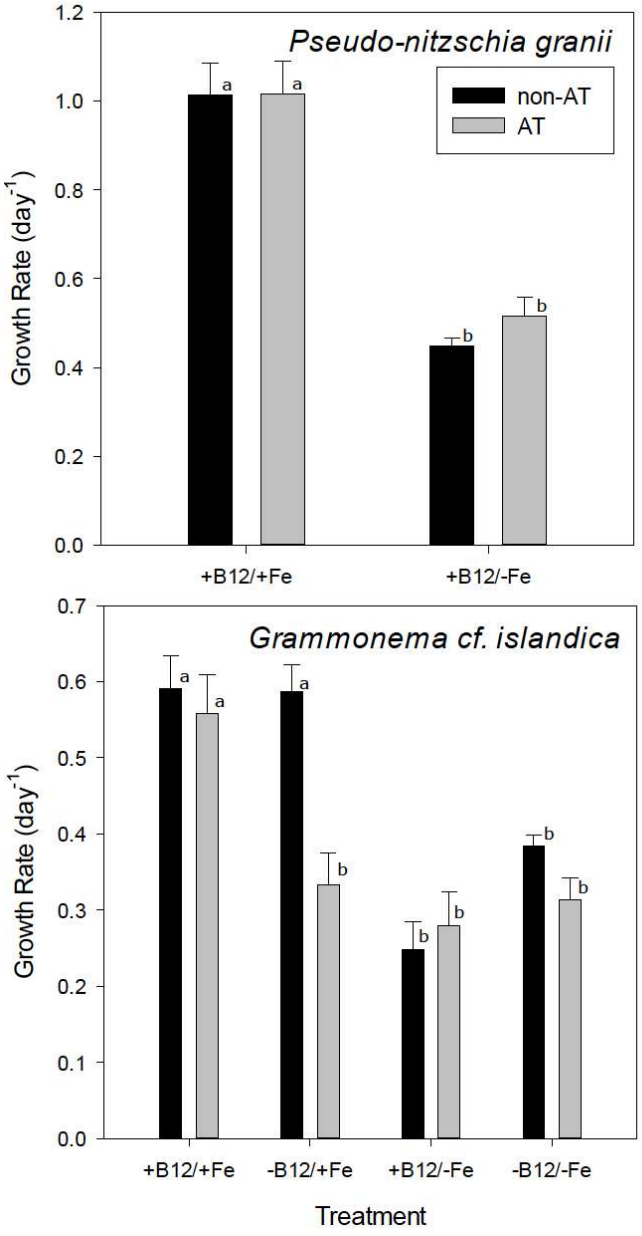

Figure 2.1. Steady-state growth rates (d^{-1}) for *P. granii* and *G. islandica* under varying Fe (+/-Fe) and vitamin B_{12} (+/-B_{12}) conditions. All treatments were grown with their natural bacterial assemblages (non-AT) and after antibiotic treatment that removed accompanying bacteria (AT).

Similarly, *P. granii* showed no significant difference in F_v/F_m between AT and non-AT cultures of the same treatment, but F_v/F_m significantly decreased between Fe-replete (+B_{12}/+Fe) and Fe-limited (+B_{12}/-Fe) treatments ($p = 2 \times 10^{-4}$ for non-AT and $p = 2 \times 10^{-4}$ for AT) (Figure

2.2). Photosynthetic cross section (σ_{PSII}) values significantly increased between Fe-replete and Fe-limited treatments, but did not significantly change between non-AT and AT cultures within the same treatment ($p = 4 \times 10^{-3}$ and $p = 6 \times 10^{-3}$) (Figure 2.3).

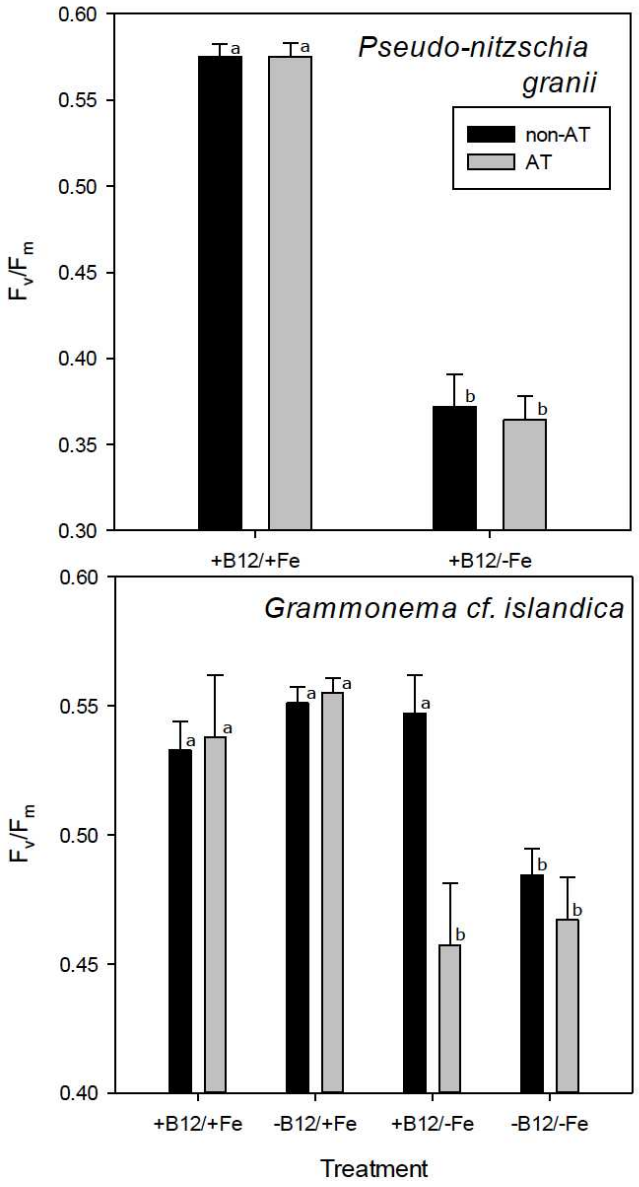

Figure 2.2. Steady-state photosynthetic efficiencies (F_v/F_m) for *P. granii* and *G. islandica* under varying Fe (+/-Fe) and vitamin B_{12} (+/-B_{12}) conditions. All treatments were grown with their natural bacterial assemblages (non-AT) and after antibiotic treatment to remove accompanying bacteria (AT). Error bars represent ±1 standard error associated with the mean (n=3). Letters indicate statistically different groupings ($p<0.05$).

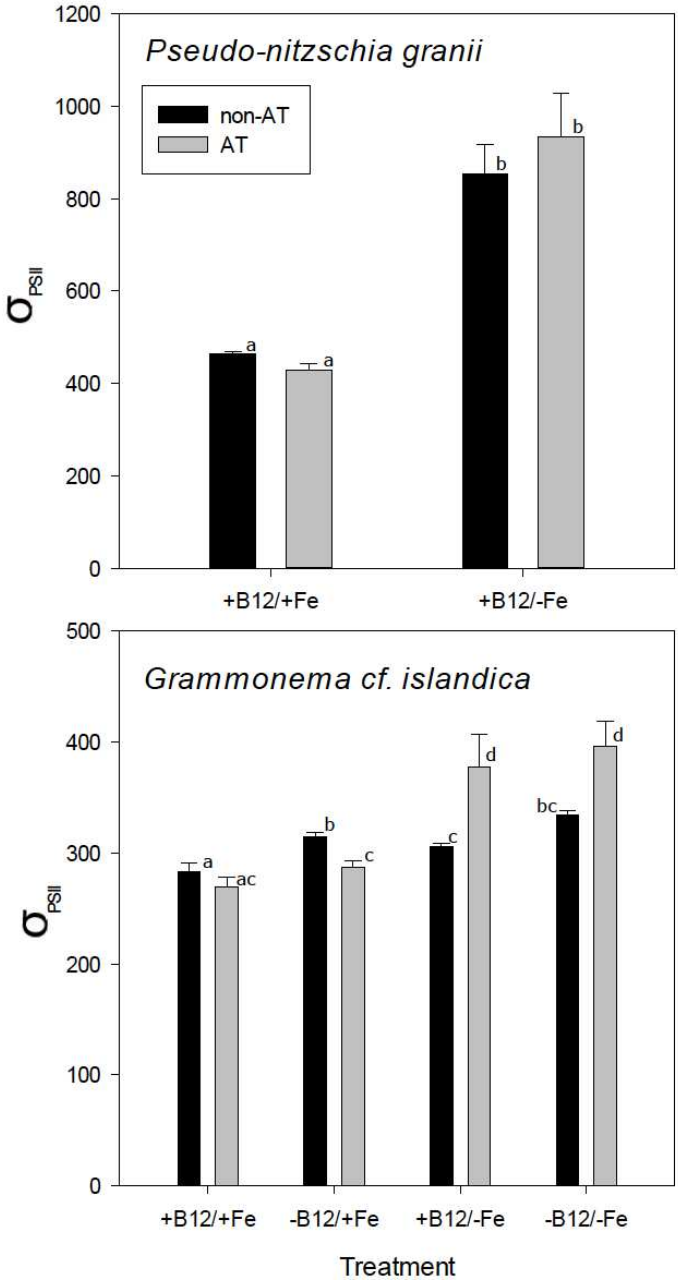

Figure 2.3. Steady-state sigma values (σ_{PSII}) for *P. granii* and *G. islandica* under varying Fe (Fe) and vitamin B_{12} (B_{12}) conditions. All treatments were grown with their natural bacterial assemblages (non-AT) as well as after antibiotic treatment that removed accompanying bacteria (AT). Error bars represent ±1 standard error associated with the mean (n=3). Letters indicate statistically different groupings ($p<0.05$).

G. islandica, in contrast to *P. granii*, showed differences in growth rate related to AT treatment between $-B_{12}$/+Fe treatments (Figure 2.1). Non-AT $-B_{12}$/+Fe growth rates were significantly higher than when the same treatment was antibiotic-treated ($p = 4 \times 10^{-4}$). When bacteria were present in Fe-replete treatments, cultures did not grow at significantly different rates. However, AT $+B_{12}$/+Fe cultures grew significantly faster than their AT $-B_{12}$/+Fe counterparts ($p = 5 \times 10^{-4}$).

Both *G. islandica* non-AT and AT $+B_{12}$/+Fe cultures and non-AT $-B_{12}$/+Fe cultures grew significantly faster than all –Fe cultures. However, AT $-B_{12}$/+Fe cultures did not grow at a significantly different rate ($p = 3 \times 10^{-3}$, $p = 1 \times 10^{-3}$, and $p = 1 \times 10^{-4}$, respectively). Changes in F_v/F_m between *G. islandica* treatments were less substantial than for *P. granii*, perhaps due to differences in how the taxa respond to Fe limitation (Suggett et al. 2009) (Figure 2.2). There were no significant differences in response between non-AT and AT *G. islandica* cultures in the same treatment except in the case of $+B_{12}$/-Fe cultures, for which F_v/F_m decreased significantly upon removal of bacteria ($p = 0.02$). Both non-AT and AT $-B_{12}$/-Fe cultures had significantly lower F_v/F_m values than their respective $-B_{12}$/+Fe counterparts ($p = 7 \times 10^{-4}$ and $p = 4 \times 10^{-4}$). σ_{PSII} values significantly decreased upon removal of bacteria from non-AT $-B_{12}$/+Fe cultures ($p = 5 \times 10^{-3}$), and increased under $-B_{12}$ conditions regardless of Fe status in non-AT cultures ($p = 6 \times 10^{-3}$, 9×10^{-4}). In contrast, AT $+B_{12}$/-Fe and AT $-B_{12}$/-Fe cultures had significantly higher σ_{PSII} values than their non-AT counterparts ($p = 0.04$ and $p = 0.049$).

Fe-Resupply Experiments

The results of Fe-resupply experiments indicated that Fe limitation slowed growth for both *P. granii* and *G. islandica*. However, only *P. granii* showed a growth response to vitamin

B_{12} limitation through reduced and non-exponential growth rates (Figure 2.4). Neither species showed an increased response to vitamin B_{12} and Fe colimitation relative to limitation of either nutrient alone.

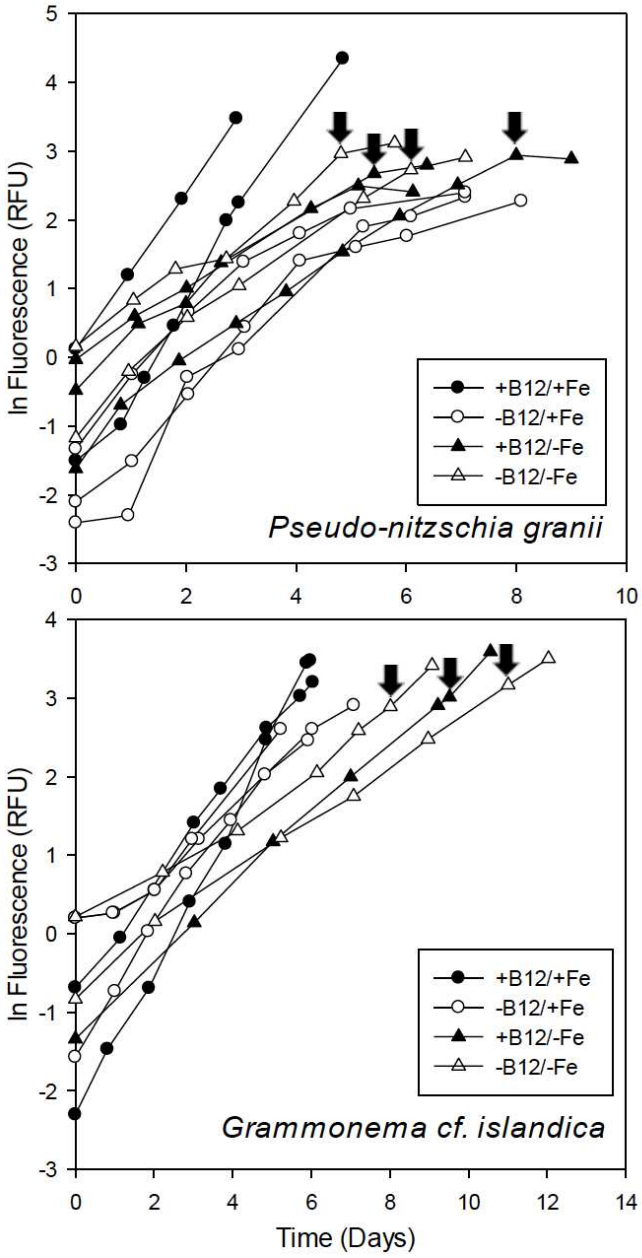

Figure 2.4. Natural log of relative fluorescence units over time for *P. granii* and *G. islandica* Fe resupply experiments. Cultures were initially grown with (+Fe) and without (-Fe) Fe while also experiencing vitamin B_{12} replete (+B_{12}) or limited (-B_{12}) conditions. Arrows indicate time of Fe resupply to previously Fe-limited cultures and color represents B_{12} status (black being +B_{12}, and white being –B_{12}). Circles denote Fe-replete cultures, while triangles denote those that originated as being Fe-limited.

P. granii cultures that were both B_{12} and Fe-replete grew exponentially and at a higher growth rate throughout all treatments than nutrient-limited cultures. Fe-limited *P. granii* cultures, both B_{12}-replete and B_{12}-limited, responded to Fe-resupply through a decrease in growth rate. In contrast, *G. islandica* $+B_{12}$ and $-B_{12}$ cultures grew at similar rates to their +Fe or –Fe counterparts, and –Fe cultures had no noticeable growth response to Fe-resupply.

Photosynthetic efficiencies did not differ significantly between Fe-replete, $+B_{12}$ and $-B_{12}$ treatments for either *P. granii* or *G. islandica* (Figure 2.5). Both species showed significantly decreased F_v/F_m values for Fe-limited treatments relative to Fe-replete treatments, regardless of B_{12}-limitation status ($p = 5 \times 10^{-3}$ and $p = 3 \times 10^{-3}$ for *P. granii* $+B_{12}$ and $-B_{12}$, $p = 3 \times 10^{-3}$ for *G. islandica* $-B_{12}$). While *P. granii* F_v/F_m for –Fe treatments increased significantly upon Fe addition ($p = 4 \times 10^{-5}$ for $+B_{12}$, $p = 0.01$ for $-B_{12}$), *G. islandica* $-B_{12}$/-Fe cultures did not respond significantly to Fe addition. Significance for $+B_{12}$/-Fe *G. islandica* cultures could not be determined. σ_{PSII} values for Fe-limited *P. granii* and *G. islandica* were significantly higher than $+B_{12}$/+Fe and $-B_{12}$/-Fe cultures ($p = 0.03$ and $p = 3 \times 10^{-4}$ for *P. granii*, and $p = 0.01$ for *G. islandica* $-B_{12}$/-Fe) and these values decreased significantly upon Fe resupply ($p = 5 \times 10^{-4}$ and $p = 3 \times 10^{-3}$ for *P. granii*; $p = 2 \times 10^{-3}$ for *G. islandica* $-B_{12}$/-Fe) (Figure 2.6). No significant difference in σ_{PSII} values was observed based on B_{12} status, either alone or in conjunction with Fe.

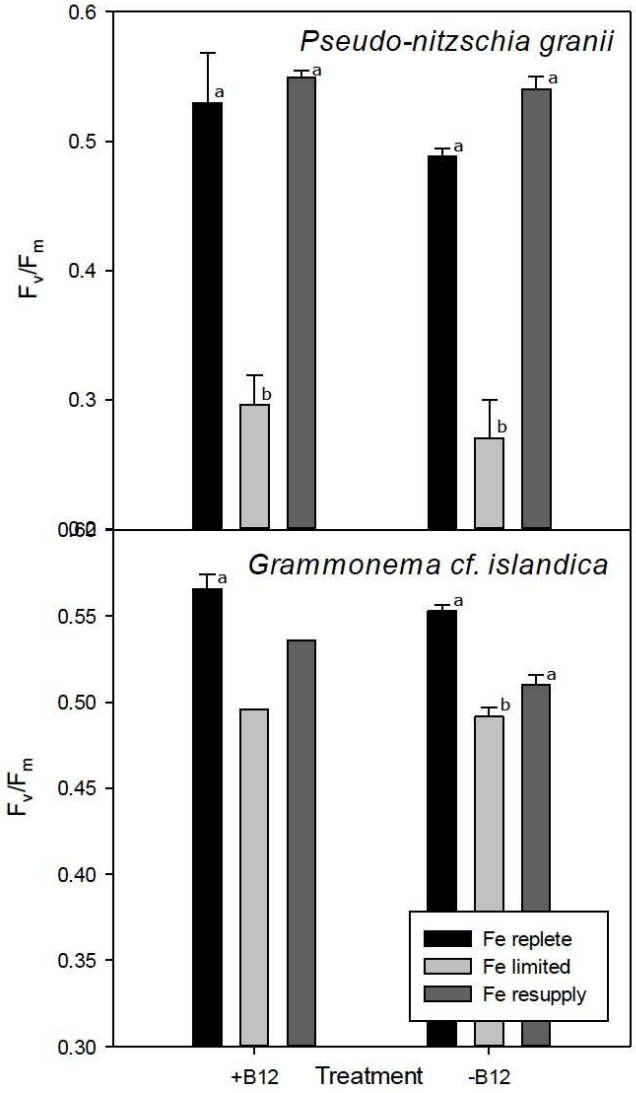

Figure 2.5. Photosynthetic efficiency (F_v/F_m) comparisons pre and post addback of Fe to Fe-limited *P. granii* and *G. islandica* cultures grown with (+B_{12}) and without (-B_{12}) vitamin B_{12}. Error bars represent ±1 standard error associated with the mean (n=3). Letters indicate statistically different groupings ($p<0.05$).

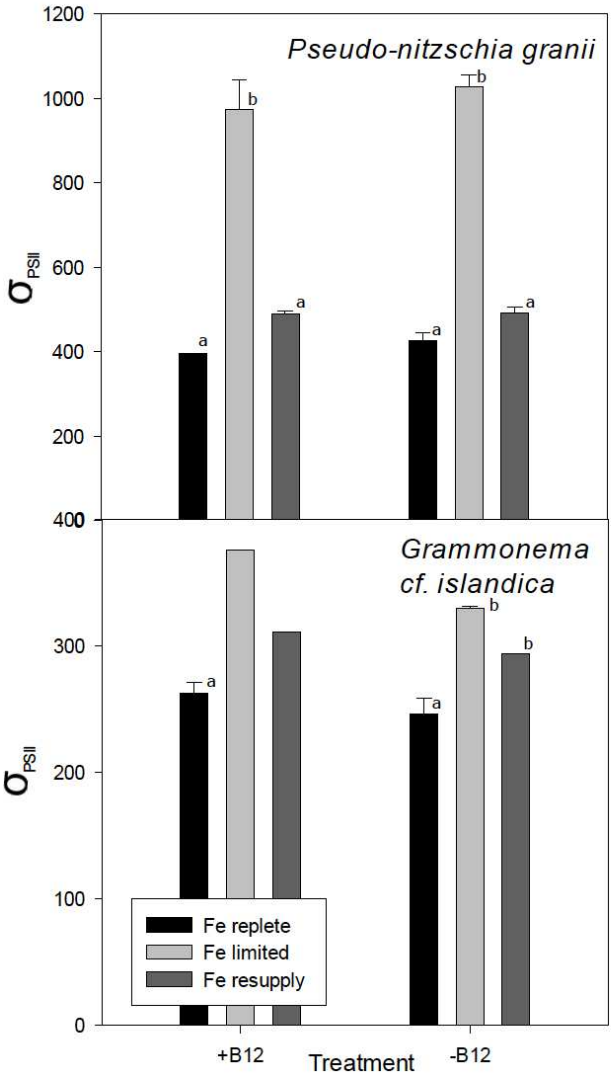

Figure 2.6. Photosynthetic cross sectional area (σ_{PSII}) comparisons pre and post addback of Fe to Fe-limited *P. granii* and *G. islandica* cultures grown with (+B_{12}) and without (-B_{12}) vitamin B_{12}. Error bars represent ±1 standard error associated with the mean (n=3). Letters indicate statistically different groupings ($p<0.05$).

Gene Expression Analysis

Gene expression analysis of *P. granii* determined that the average ratio of MetH/ACT transcript copies ranged from 1.96 ± 0 .20 for –B_{12}/+Fe steady state cultures to 0.27 ± 0.04 for +B_{12}/+Fe steady state cultures (Figure 2.7A). MetH/ACT was significantly higher under B_{12}-

limitation (-B_{12}/+Fe) relative to nutrient-replete cultures (+B_{12}/+Fe) ($p = 7 \times 10^{-3}$). Significance of vitamin B_{12} and Fe colimited cultures could not be determined because of a lack of replication, but similar trends were observed. Expression of MetH/ACT decreased from pre to post Fe-resupply in +B_{12}/-Fe and –B_{12}/-Fe cultures. There was no significant difference in MetH/ACT between cultures experiencing nutrient limitation, regardless of whether vitamin B_{12}, Fe, or both were limiting growth.

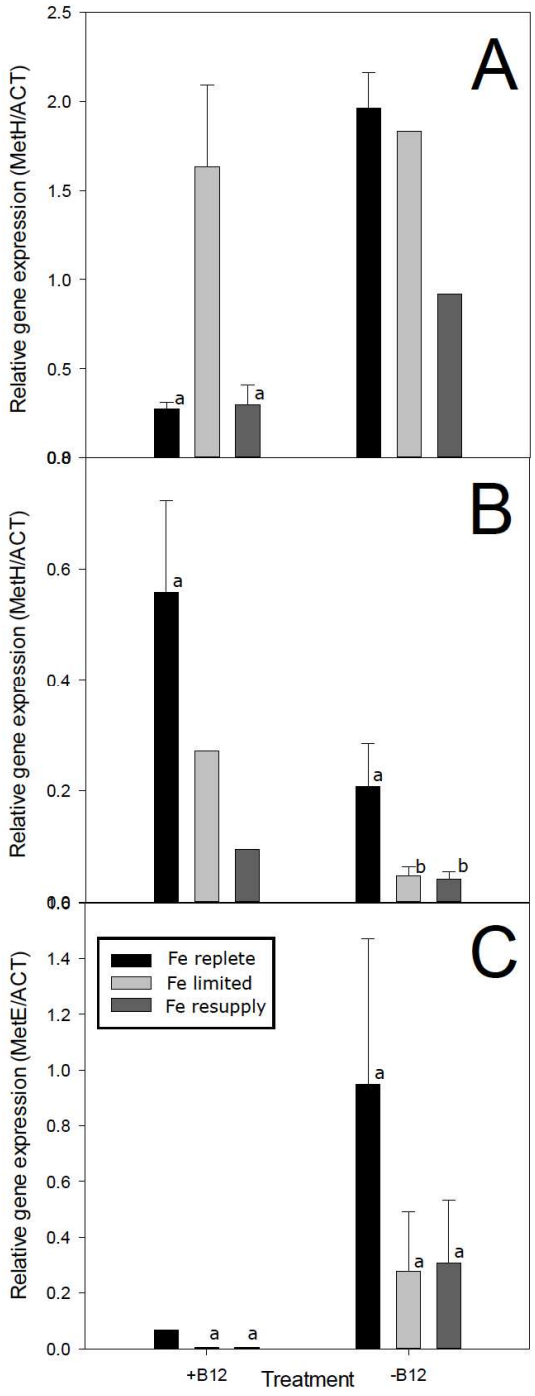

Figure 2.7A-C. Relative gene expression of A) *P.granii* MetH, B) *G. islandica* MetH and C) *G. islandica* MetE under Fe-replete, Fe-limited and Fe-resupplied Fe-limited cells grown with ($+B_{12}$) and without ($-B_{12}$) vitamin B_{12}. All genes are normalized to Actin (ACT) transcripts. Error bars represent ±1 standard error associated with the mean ($n \geq 3$). Letters indicate statistically different groupings ($p<0.05$).

Expression patterns for *G. islandica* MetH/ACT differed from that of *P. granii* in that nutrient limitation decreased relative expression rather than increasing it (Figure 2.7B). Expression ratios ranged from 0.56 ± 0.17 for +B_{12}/+Fe cultures to 0.041 ± 0.02 for –B_{12}/-Fe cultures. MetH/ACT expression decreased under vitamin B_{12} limitation (-B_{12}/+Fe) and Fe limitation (+B_{12}/-Fe) compared to replete cultures (+B_{12}/+Fe). However, MetH/ACT decreased further upon Fe resupply to +B_{12}/-Fe cultures. The lowest expression levels were seen in vitamin B_{12} and Fe colimited cultures, both before and after Fe resupply. These MetH/ACT ratios were lower than those of replete cultures, as well as cultures limited by vitamin B_{12} alone.

MetE/ACT in *G. islandica* ranged from 0.95 ± 0.52 in –B_{12}/+Fe treatments to 0.0005 in +B_{12}/-Fe post Fe resupply (Figure 2.7C). Expression was higher in Fe-replete, B_{12}-limited cultures than in cultures replete with both nutrients. Expression was highly downregulated in cultures experiencing solely Fe limitation (+B_{12}/-Fe) compared to nutrient replete cultures (+B_{12}/+Fe), both pre and post Fe resupply. Expression of MetE/ACT was increased in B_{12} and Fe colimited cultures, both pre and post Fe resupply, but was not higher than when B_{12} alone was limiting.

Chlorophyll a quota analysis

Both *P. granii* and *G. islandica* decreased chlorophyll *a* quotas (pg chl *a* per cell) under vitamin B_{12} limitation (Figure 2.8). Both taxa also significantly decreased chl *a* quotas even further under Fe limitation, regardless of B_{12} status ($p = 6 \times 10^{-4}$ for +B_{12} *P. granii*; $p = 0.01$ for –B_{12} *G. islandica*) and increased chl *a* per cell after Fe resupply to a lesser extent. No combined effect of vitamin B_{12} and Fe colimitation was observed for either diatom species.

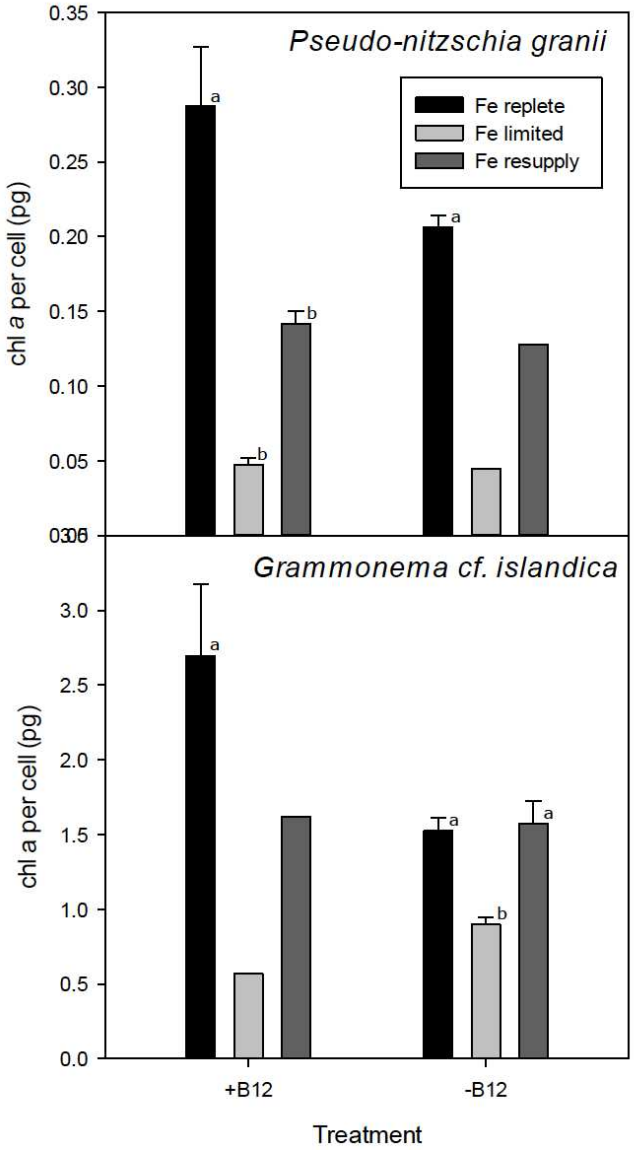

Figure 2.8. Chlorophyll *a* quotas (pg/cell) for vitamin B_{12} replete ($+B_{12}$) and limited ($-B_{12}$) cultures grown under Fe-replete, Fe-limited, and post Fe-resupply conditions. Error bars represent ±1 standard error associated with the mean ($n \geq 2$). Letters indicate statistically different groupings ($p<0.05$).

Discussion

In Chapter 1, we demonstrated that the presence or absence of a single gene, MetE, determines whether diatom species are auxotrophic for vitamin B_{12}. However, algae rely on more than just B_{12}; they are entwined in a web of biotic and abiotic interactions that can alter their nutrient requirements and relative fitness. Another one of these factors is Fe, which limits primary production in large areas of the world's oceans (Watson et al. 1995). Vitamin B_{12} can be intermittently colimiting in these HNLC regions, and by examining the intersection of these nutrient requirements we can develop a more complete understanding of how their availability can affect community succession during diatom blooms.

This study shows that although both Fe and vitamin B_{12} can affect diatom growth, photosynthetic health, and chlorophyll *a* content, there is little to suggest that colimitation acts synergistically. It is only in gene expression patterns of MetH and MetE that any Fe-B_{12} colimitation effect may be indicated. Whether these gene expression patterns result in differences in competitive ability between different diatoms under Fe-B_{12} colimitation requires further research.

Similar patterns in growth and gene expression were seen in *P. granii*, a B_{12}-auxotroph, and *G. islandica*, which possesses MetE, as seen in Chapter 1 of this thesis. Iron limitation also affected cultures as would be expected from previous studies (Raven 1988, Greene et al 1991), decreasing growth rates and affecting changes in photosynthetic efficiencies (F_v/F_m) relative to nutrient-replete cultures. Photosynthetic efficiencies decreased because as Fe becomes scarce, the proportion of incoming energy being utilized by the photosynthetic electron transport (PET) chain (F_v/F_m) decreases. This is because an estimated 80% of the Fe required by phytoplankton is utilized in PET (Raven 1990). When Fe-limited, diatoms produce fewer chloroplasts and reduce

chlorophyll *a* content, which is also consistent with the results of this study (Davey and Geider 2001).

Generally, the presence or absence (non-AT and AT treatments) of bacteria in steady-state cultures did not significantly affect photosynthetic efficiencies. However, B_{12}-replete and Fe-limited *G. islandica* did not demonstrate a significant reduction in F_v/F_m until after antibiotic treatment (AT). Likewise, under Fe-limitation, *G. islandica* sigma (σ_{PSII}) did not increase until cultures were treated with antibiotics to remove bacteria. In this case, bacteria may be facilitating photosynthetic health in an Fe-specific way, possibly related to siderophore excretion and usage (Amin et al. 2012).

While Fe had similar effects on *P. granii* and *G. islandica*, the effects of B_{12}-limitation were more varied. Presence or absence of the culture's natural bacterial assemblages did not significantly impact steady-state growth rates except in the case of B_{12}-limited, Fe-replete *G. islandica*, in which growth rates decreased by half once bacteria were removed. This is consistent with previous studies, which have shown that phytoplankton must obtain their vitamin B_{12} from exogenous bacterial and archaeal sources (Croft et al. 2005), and in their absence must utilize MetE to continue growth.

B_{12}-limited *P. granii* cultures could not grow in steady-state, regardless of whether they had been antibiotic treated. This could be indicative either of an assemblage lacking in B_{12}-synthesizers, higher B_{12} quotas, or a combination of both factors. As *P. granii* has been in culture for a relatively long time (since 2010), mostly in vitamin-replete medium, there has been time for the diatom's bacterial assemblage to be altered. B_{12} auxotrophy is selected for evolutionarily as well as being competitively advantageous in environments where B_{12} is replete, and it is

therefore likely that B_{12}-synthesizers in the culture would eventually be outcompeted by auxotrophs (Helliwell et al. 2015).

Although B_{12} status did not significantly affect photosynthetic efficiencies, B_{12}-limitation decreased chl *a* content of affected cells. This phenomenon, called chlorosis, is a common symptom of nutrient deficiency and this study's findings show that B_{12}-deficiency causes similar effects as other nutrients (Doucette and Harrison 1990, Greene et al. 1991, 1992). It has previously been hypothesized that B_{12} and Fe could interact within the photosynthetic apparatus through phylloquinone (vitamin K), an electron carrier in photosystem I that requires S-adenosylmethionine (which is B_{12}-dependent) for its creation. Vitamin B_{12} limitation was observed to impair photosynthesis when Fe was not available (Lohmann et al 2006, King et al 2011). However, none of the variables examined in this study demonstrated a combined Fe and B_{12} effect on photosynthetic processes.

Iron and B_{12} limitation separately decreased the chl *a* content of cells, and 24 hours after Fe resupply these cultures had not reached chl *a* concentrations of nutrient replete cultures. In addition, Fe-limited *P. granii* cultures showed decreased growth rates 24 hours after Fe resupply, indicating that cell division rates had not yet started to increase in response to Fe addition. Previous studies have found that when supplied with Fe, cells used it in essential Fe-requiring systems to restore core functions before utilization in cellular division (Davey and Geider 2001). Chl *a* contents and growth rates indicate that previously Fe-limited cultures may not have fully recovered from Fe stress by the end of this study's experiments. Although F_v/F_m and sigma (σ_{PSII}) measurements indicated that Fe resupply was largely successful in allowing cultures to increase photosynthetic efficiencies, this is merely one component of the recovery from Fe limitation.

Gene expression results corroborate the idea that cells had yet to fully recover from Fe limitation. Except in the case of *P. granii* B_{12}-replete MetH, gene expression ratios after Fe resupply more closely matched Fe-limited ratios than those of replete cultures. This delay in gene expression change was also seen in Marchetti et al. (2012), where diatoms were found to still be expressing gene transcripts indicative of an Fe-limited community 98 hours after Fe resupply. This lack of immediate response could be a strategy that helps *P. granii* and *G. islandica*, both of which were isolated from the HNLC Station Papa in the northeast Pacific, to survive during transient Fe fluxes (Marchetti et al. 2012). Alternatively, methionine synthase's primary purpose in the creation of methionine, an amino acid essential to DNA synthesis, could play a role. Perhaps when cellular division is slowed during Fe stress, gene expression for these division-related genes is also downregulated.

From the results of this study, it seems that upregulated MetE is a good predictor of whether vitamin B_{12} is limiting in an environment, although this effect may be less pronounced when Fe and B_{12} are colimiting. In a metatranscriptomic study of diatom response to Fe fertilization, MetE was found to be significantly upregulated in the community after Fe fertilization (Marchetti et al. 2012). This could have been because of a link between the two nutrients at the molecular level or because vitamin B_{12} became limiting as diatom blooms formed. This study indicates that increased expression of MetE is generally not tied to Fe status, but rather is indicative of whether B_{12} is available. Colimitation may decrease MetE expression because of slowed cell division, as previously mentioned. Since MetE usage requires approximately 30-fold more nitrogen than MetH and because nitrate reductase is slowed under Fe limitation, MetE may not be able to obtain the large quantities of nitrate needed to function

optimally (Timmermans et al. 1994, 1998, Bertrand and Allen 2012). The results of this study indicate that it is likely B_{12} became a limiting nutrient during the course of these incubations.

It has been previously shown, both in Chapter 1 as well as in previous studies (Croft et al. 2005), that the vitamin B_{12} auxotrophy in diatoms has the possibility to alter bloom dynamics when B_{12} becomes variable or limiting. Adding Fe into this picture, it seems, results in separate nutrient limitation effects that do not behave synergistically. Although changes in gene expression were observed among both *P. granii* and *G. islandica* and on longer timescales may impact cells physiologically, over the timescale this study was conducted the primary effect of B_{12} and Fe limitation was to follow physiological patterns of Fe limitation regardless of B_{12} status.

Since MetE is present in less than half of examined algae (Croft et al. 2005), using it alone as a molecular indicator could fail to identify B_{12} limitation when few algae possessing MetE are present in the phytoplankton community. However, this study indicates that MetE could still prove to be a reliable molecular indicator of B_{12} limitation, and would not be confounded by Fe limitation.

During natural cycles of Fe limitation and fertilization in the ocean, tradeoffs between diatoms such as B_{12}-auxotroph *P. granii*, which shows a great deal of flexibility under Fe stress, and the MetE-possessing, but Fe limitation-intolerant *G. islandica*, would determine which diatom is able to outcompete the other. This may serve as an example of the "paradox of the plankton," demonstrating how diatoms living in the same area can both thrive when they occupy different niches in the ever-changing marine environment (Hutchinson 1961). Even over small spatial and temporal scales, vitamin B_{12} has been shown to vary substantially in concentration

(Sañudo-Wilhelmy et al 2012) and these diatoms may have adapted to survive under distinct regimes of B_{12} and Fe limitation in order to coexist.

APPENDIX 1: PRIMER INFORMATION

Appendix 1: Primer Sequences. Primer sequences developed as part of this study. Forward (F) and reverse (R) sequences shown for *P. granii*, *F. cylindrus,* and *Grammonema cf. islandica* MetH, MetE, and Actin (ACT) genes when applicable.

Diatom	MetH	MetE	ACT
Pseudo-nitzschia granii	F:5'-AAAGATCGCCAACGACATTC-3' R:4'-GAAGGAGAAAGCAGCAATCG-3'	N/A	F: 5'-GGACATCTGAATCGCTCGTTT-3' R: 5'-ACTCGTTGACTACCACCGCT-3'
Fragilariopsis cylindrus	F: 5'-ATGCCGACCGTAAAAAGATG-3' R: 5'-AATCCATTGCACTCCCGTAG-3'	F: 5'-TTACGGGACCAATCACCATT-3' R: 5'-CAACTGCCCACCTGAGGTAT-3'	F: 5'-ATTGTTGCTCCTCCAGAACG-3' R: 5'-GGTGAACGATAGATGGACCAG-3'
Grammonema cf. islandica	F: 5'-AGCCTCGGAGGTAGGAAGAG-3' R: 5'-GGCAACTGAAGACATGCTGA	F: 5'-CTGGAACGACACCCAGAAAT-3' R: 5'-GAAGCACTGGAAAGGTCAGC-3'	F: 5'-AGTTGTTGCTTCGTCGGTCT-3' R: 5'-GATAGCTCGACTGCCTGACC-3'

APPENDIX 2: MetE SUPPLEMENTARY INFORMATION

Appendix 2A: Protist Organism ID's and Diatom MetE Transcript Copies. Identification information for protists found to possess MetE according to BLAST analysis (e > 1E-5) and MetE contig paired aligned read counts (transcript copies) from diatom transcriptomes sequenced as part of the MMETS project and deposited in the CAMERA database, along with Genbank accession numbers for the MetE genes of organisms used for culture experiments in this study. "*" denotes species with MetE gene sequences too short (<600aa) to be used in phylogenetic analysis.

Species	Strain	MMETSP Organism ID	MMETSP Contig ID	Genbank Accession Number	Transcript Copies	e Value
Gymnochlora sp.	CCMP2014	110	4032			0
Partenskyella glossopodia	RCC365	1318	67662			0
Dunaliella tertiolecta	CCMP1320	1126	4123			0
Picocystis salinarum	CCMP1897	807	3907			0
Stichococcus sp.	RCC1054	1473	2104			0
Vitrella brassicaformis	CCMP3346	1451	1997			0
Alveolata sp.	CCMP3155	288	1262			0
Amphiprora sp.	CCMP467	724	18442		1330	0
Aplanochytrim sp.	PBS07	956	2331			0
Astrosyne radiata	13vi08-1A	418	15325		435	0
Attheya septentrionalius	CCMP2084	1449	6604		659	0
Chaetoceros debilis	MM31A-1	150	59761			0
Corethron hystrix	308	10	9667		588	0
Corethron pennatum	L29A3	171	12449			0
Fragilariopsis kerguelensis	L26-C5	733	49273	KJ866918	584	0
Fragilariopsis kerguelensis	L2-C3	906	161813			0
Proboscia alata	PI-D3	174	22718		780	0
Proboscia inermis	CCAP1064/1	816	21562		1049	0
Staurosira complex sp.	CCMP2646	1361	6012		1673	0

Thalassionema nitzschioides	L26-B	156	43459	763	0
Madagascaria erythrocladiodes	CCMP2084	1450	20222		0
Rhodosorus marinus	UTEX LB2760	315	7163		0
Lotharella globosa	LEX01	41	9678		3.00E-176
Chromera velia	CCMP2878	290	779		8.00E-170
Chlamydomonas euryale	CCMP19	63	12838		4.00E-169
Glenodinium foliaceum	CCAP1116_3	119	27434		2.00E-160
Schizochytrium aggregatum	ATCC28209	964	36		9.00E-157
Heterosigma akashiwo	NB	415	385539		7.00E-152
Ochromonas sp.	CCMP1899	1177	16665		4.00E-148
Picochlorum oklahomensis	CCMP2329	1161	17088		1.00E-147
Goniomonas pacifica	CCMP1869	108	16184		1.00E-147
Polytomella parva	SAG63-3	52	11319		3.00E-137
*Paraphysomonas imperforata**	PA2	103	19330		3.00E-116
Heterosigma akashiwo	CCMP3107	410	4807		7.00E-116
*Minutocellus polymorphus**	NH13	1070	23373	65	7.00E-109
Hemiselmis andersenii	CCMP644	43	3921		5.00E-86
*Amphiprora paludosa**	CCMP125	1065	7947	65	3.00E-40
Pteridomonas danica	PT	101	194		3.00E-37
*Pinguiococcus pyrenoidosus**	CCMP2078	1160	31786		3.00E-31
*Cryptomonas paramecium**	Unknown	38	8426		1.00E-27
Vannella sp.	DIVA3	168	14527		2.00E-27
*Aulacoseira subarctica**	CCAP1002/5	1064	50128	7	3.00E-21
*Karenia brevis**	Wilson	648	25770		6.00E-18
Ceratium fusus	PA161109	1074	213620		7.00E-18
*Karenia brevis**	SP1	574	38347		7.00E-18
*Karenia brevis**	CCMP2229	27	10955		8.00E-18

*Karenia brevis**	SP3	528	30976			1.00E-16
*Paramoeba atlantica**	621/1	151	26423			4.00E-13
Scrippsiella trochoidea	CCMP3099	271	101678			2.00E-12
*Karlodinium micrum**	CCMP2283	1015	5544			2.00E-12
Pterosperma sp.	CCMP1384	1438	23442			7.00E-12
Brandtodinium nutriculum	RCC3387	1462	88403			3.00E-10
*Stereomyxa ramosa**	Chinc5	439	47738			4.00E-10
Fragilaria/Grammonema sp.	UBC1301					
*Chaetoceros sp.**	UNC1202	1429	60215	KJ866914	4	
Fragilariopsis cylindrus	CCMP1102			KJ866917		
Navicula lanceolata	UNC1404					
Phaeodactylum tricornutum	CCAP1055/1					
*Actinocyclus actinochilus**	UNC1403					
*Chaetoceros rostratus**	UNC1408					
*Proboscia alata**	UNC1405					
*Thalassiosira antarctica**	UNC1401					

Appendix 2B: Alignment of MetE sequences obtained from selected available diatom genomes and transcriptomes. MetE from *F. cylindrus* (CCMP1102) is used as the reference. Darker colors indicate columns of high consensus between aligned species, while lighter color indicates areas of low consensus.

APPENDIX 3: SYBR STAINING RESULTS

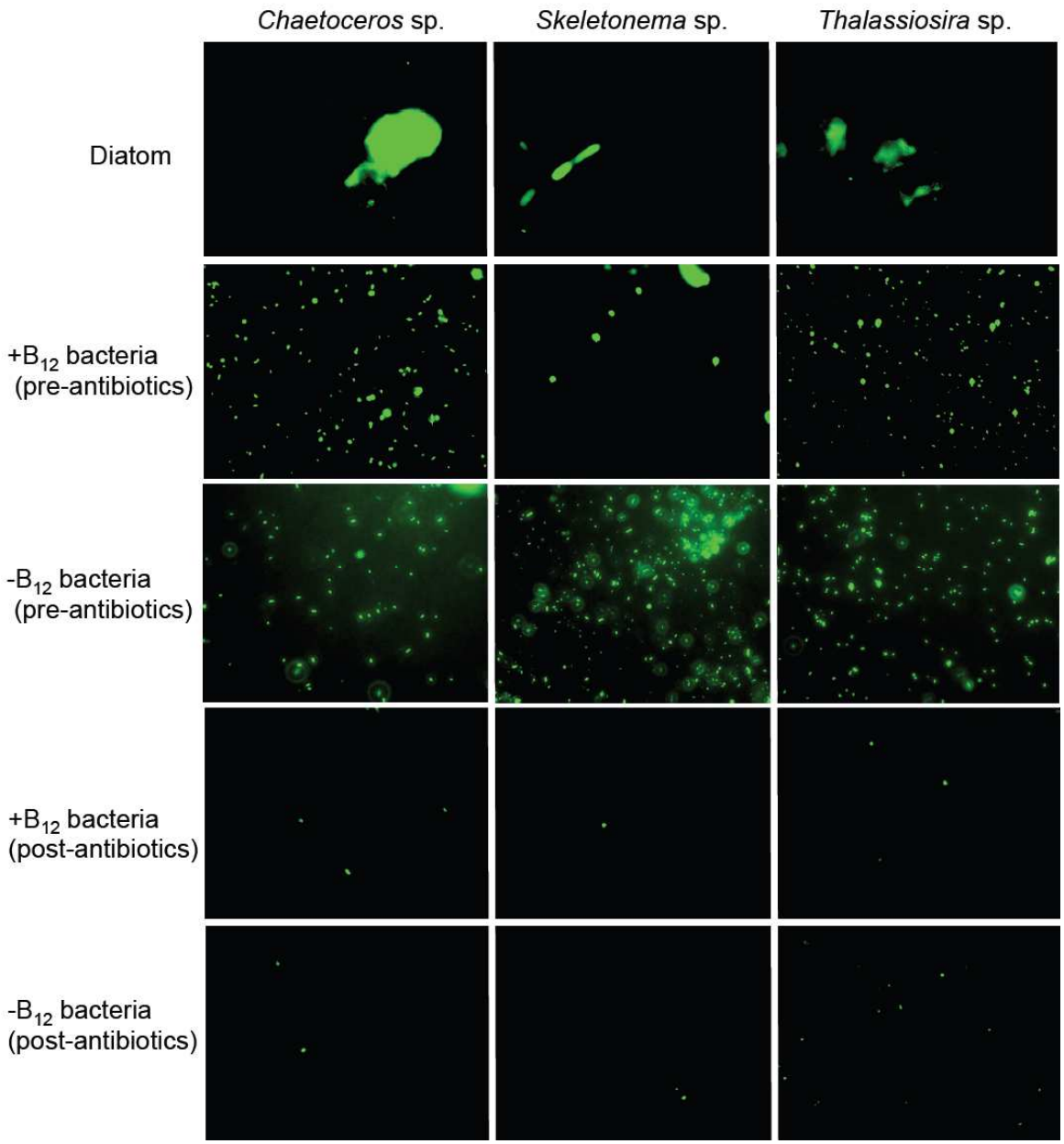

Appendix 3: Epifluorescent microscopy images (100x) of SYBR-stained +B_{12} and –B_{12} *Chaetoceros* sp., *Skeletonema* sp, and *Thalassiosira* sp. cultures with and without antibiotic treatment.

APPENDIX 4: DIATOM LOCATION INFORMATION

Appendix 4: Diatom location information. Latitude and longitude for diatom species utilized in MetE biogeography map. Data courtesy of C. Moreno.

Genus	Species	Strain	MMETSP ID	Latitude	Longitude
Asterionellopsis	glacialis	CCMP134	MMETSP0705	32.655	-117.14
Asterionellopsis	glacialis	CCMP1581	MMETSP1394	51.7333	3.7667
Asterionellopsis	glacialis	Unknown	MMETSP0713	41.325	-70.5667
Cyclophora	tenuis	ECT3854	MMETSP0397	21.514	-157.8362
Licmophora	paradoxa	CCMP2313	MMETSP1360	42.41915	-70.91349
Staurosira	complex sp.	CCMP2646	MMETSP1361	-36.5062	-73.1225
Synedropsis	recta cf	CCMP1620	MMETSP1176	-77.8333	163
Thalassionema	frauenfeldii	CCMP 1798	MMETSP0786	18.47	-64.575
Thalassionema	nitzschioides		MMETSP0693	41.325	-70.5667
Thalassiothrix	antarctica	L6-D1	MMETSP0152	-51.83333	-28.66667
Thalassionema	nitzschioides	L26-B	MMETSP0156	-47.86667	-15.8
Chaetoceros	affinis	CCMP159	MMETSP0088	29.42	-86.105
Chaetoceros	brevis	CCMP164	MMETSP1435	-61.2833	-54.7361
Chaetoceros	curvisetus	Unknown	MMETSP0716	32.9	-117.255
Chaetoceros	debilis	MM31A-1	MMETSP0150	-49.6	2.1
Chaetoceros	dichaeta	CCMP1751	MMETSP1447	-49.9	11.55
Chaetoceros	neogracile	CCMP1317	MMETSP0751	32.85	-117.35
Chaetoceros	sp.	UNC1202	MMETSP1429	48.816	-128.666
Cyclotella	meneghiniana	CCMP 338	MMETSP1057	43.8442	-69.641
Dactyliosolen	fragilissimus	Unknown	MMETSP0580	41.325	-70.5667
Ditylum	brightwellii	GSO103	MMETSP1002	49.654	-127.436
Ditylum	brightwellii	GSO104	MMETSP1010	41.325	-70.57
Ditylum	brightwellii	GSO105	MMETSP0998	47.74	-122.417
Eucampia	antarctica	CCMP1452	MMETSP1437	-77.8333	163
Extubocellulus	spinifer	CCMP396	MMETSP0696	31.3172	-113.56
Helicotheca	tamensis	CCMP826	MMETSP1171	30	-60
Minutocellus	polymorphus	CCMP3303	MMETSP1434	-17.5	11.25
Skeletonema	dohrnii	SkelB	MMETSP0562	41.57361	-71.40861
Skeletonema	grethea	CCMP 1804	MMETSP0578	41.4331	-71.455
Skeletonema	japonicum	CCMP2506	MMETSP0593	34.3	132.4
Skeletonema	marinoi	FE60	MMETSP1040	43.5	14.5
Skeletonema	marinoi	FE7	MMETSP1039	43.5	14.5
Skeletonema	marinoi	SM1012Hels-07	MMETSP0319	59.51	23.15
Skeletonema	marinoi	UNC1201	MMETSP1428	48.816	-128.666
Skeletonema	marinoi	skelA	MMETSP0918	41.5736105	-71.4086105
Skeletonema	menzelii	CCMP793	MMETSP0603	41.566	-70.5842
Attheya	septentrionalis	CCMP2084	MMETSP1449	77.8136	-76.3697
Chaetoceros	cf. neogracile	RCC1993	MMETSP1336	70.68333333	-138.3666667
Detonula	confervacea	CCMP 353	MMETSP1058	41.6	-71.18333333

Minutocellus	polymorphus	RCC2270	MMETSP1322	71.18333333	-159.4166667
Triceratium	dubium	CCMP147	MMETSP1175	30	-60
Corethron	pennatum	L29A3	MMETSP0171	-47.33333	-15.65
Coscinodiscus	wailesii	CCMP2513	MMETSP1066	31.4322	-80.358
Leptocylindrus	danicus var. apora	B651	MMETSP0322	40.8083	14.25
Leptocylindrus	danicus var. danicus	B650	MMETSP0321	40.8083	14.25
Leptocylindrus	danicus	CCMP1856	MMETSP1362	25	-90
Nitzschia	punctata	CCMP561	MMETSP0744	32.99	-117.255
Proboscia	alata	PI-D3	MMETSP0174	-64.0038	-0.0025
Proboscia	inermis	CCAP1064/1	MMETSP0816	-63.25	-58.3333
Pseudo-nitzschia	arenysensis	B593	MMETSP0329	40.8083	14.25
Pseudo-nitzschia	delicatissima	B596	MMETSP0327	40.8083	14.25
Rhizosolenia	setigera	CCMP 1694	MMETSP0789	23.5643	58.853
Skeletonema	marinoi	SM1012Den-03	MMETSP0320	55.5837	12.412
Thalassiosira	antarctica	CCMP982	MMETSP0902	59.5	10.6
Thalassiosira	gravida	GMp14c1	MMETSP0492	41.92732	-67.85788
Thalassiosira	miniscula	CCMP1093	MMETSP0737	32.9	-117.255
Thalassiosira	oceanica	CCMP1005	MMETSP0970	33.1833	-65.25
Thalassiosira	punctigera	Tpunct2005C2	MMETSP1067	47.6901	-122.40041
Thalassiosira	rotula	CCMP3096	MMETSP0403	49.65	-127.4338
Thalassiosira	rotula	GSO102	MMETSP0910	48.629353	-122.957542
Thalassiosira	sp.	FW	MMETSP1059	34.27944	-114.22222
Thalassiosira	weissflogii	CCMP1010	MMETSP1405	37	-65
Thalassiosira	weissflogii	CCMP1336	MMETSP0878	41.11	-72.1
Amphiprora	paludosa	CCMP125	MMETSP1065	41.525	-70.6736
Amphiprora	sp.	CCMP467	MMETSP0724	32.9	-117.255
Amphora	coffeaeformis	CCMP127	MMETSP0316	41.525	-70.6736
Entomoneis	sp.	CCMP2396	MMETSP1443	77.8333	-75.55
Fragilariopsis	cylindrus	CCMP1102		-64.08	-48.7033
Fragilariopsis	kerguelensis	L2-C3	MMETSP0906	-48.1	-24.25
Fragilariopsis	kerguelensis	L26-C5	MMETSP0733	-48	-16
Fragilariopsis	radiata	13vi08-1A	MMETSP0418	13.4427	144.6428
Pseudo-nitzschia	delicatissima	UNC1205	MMETSP1432	48.816	-128.666
Pseudo-nitzschia	fraudulenta	WWA7	MMETSP0850	34.0847	-119.05
Pseudo-nitzschia	granii	UNC1204		50	-145
Pseudo-nitzschia	heimii	UNC1101	MMETSP1423	50	-145
Pseudo-nitzschia	pungens	cf. cingulata	MMETSP1060	47.6901	-122.40041
Pseudo-	pungens	cf. pungens	MMETSP1061	47.6901	-122.40041

nitzschia Stauroneis	constricta	CCMP1120	MMETSP1352	-0.7475	-126.03

REFERENCES

Alexander H, Jenkins B, Rynearson T, Saito M, Mercier M, Dyhrman S (2012) Identifying reference genes with stable expression from high throughout sequence data. Front Aquat. Microbiol. 3:385.

Amin S.A, Parker MS, Armbrust EV (2012) Interactions between diatoms and bacteria. Microbiol. Mol. Biol. Rev. 76:667–84.

Appaji RN, Ambili M, Jala VR, Subramanya HS, Savithri HS (2003). Structure-function relationship in serine hydroxymethyltransferase. Biochim. Biophys. Acta 1647: 24–9.

Armbrust EV, Berges JA, Bowler C, Green BR, Martinez D, et al. The genome of the diatom *Thalassiosira pseudonana*: ecology, evolution, and metabolism. Science 306: 79-86, doi: 10.1126/science.1101156

Assmy P, Smetacek V, Montresor M, Klaas C, Henjes J, Strass VH, *et al*. (2013) Thick-shelled, grazer-protected diatoms decouple ocean carbon and silicon cycles in the iron-limited Antarctic Circumpolar Current. PNAS 110: 20633-20638.

Baines SB, Twining BS, Brzezinski MA, Nelson DM, Fisher NS (2010) Causes and biogeochemical implications of regional differences in silicification of marine diatoms. Global Biogeochem. Cycles. 24:GB4031.

Banerjee R and RM (1990) Cobalamin-dependent methionine synthase. FASEB J. 4:1450–9.

Bertrand EM, Saito MA, Rose JM, Riesselman CR, Noble AE, Lee PA, Ditullio GR (2007) Vitamin B_{12} and iron colimitation of phytoplankton growth in the Ross Sea. Limnol. Oceanogr. 52:1079–93.

Bertrand, EM, MA Saito, YJ Jeon, and BA Neilan. 2011. Vitamin B_{12} biosynthesis gene diversity in the Ross Sea: the identification of a new group of putative polar B_{12} synthesizers. Environ. Microbiol. 13: 1285-1298. doi: 10.1111/j.1462-2920.2011.02428.x

Bertrand, EM, Allen AE (2012) Influence of vitamin B auxotrophy on nitrogen metabolism in eukaryotic phytoplankton. Front. Microbiol. 3:Article 375, pages 1–16.

Bertrand, EM, AE Allen, CL Dupont, TM Norden-Krichmar, J. Bai, R.E. Valas, and M.A. Saito. 2012. Influence of cobalamin scarcity on diatom molecular physiology and identification of a cobalamin acquisition protein. PNAS 109: E1762-1771. doi: 10.1073/pnas.1201731109

Bertrand, EM, Moran DM, Mcilvin MR, Hoffman JM, Allen AE, Saito MA (2013) Methionine synthase interreplacement in diatom cultures and communities : Implications for the persistence of B_{12} use by eukaryotic phytoplankton. Limnol. Oceanogr. 58:1431–50.

Bonnet, S, Webb EA, Panzeca C, Karl DM, Capone DG, Sañudo-Wilhelmy SA (2010) Vitamin B_{12} excretion by cultures of the marine cyanobacteria Crocosphaera and Synechococcus. Limnol. Oceanogr. 55:1959–64.

Boyd PW, Watson AJ, Law CS, Abraham ER, Trull T, Murdoch R, Bakker DC, et al. (2000) A mesoscale phytoplankton bloom in the polar Southern Ocean stimulated by iron fertilization. Nature. 407:695–702.

Boyd PW, Jickells T, Law CS, Blain S, Boyle EA, Buesseler KO, Coale KH, et al. (2007) Mesoscale iron enrichment experiments 1993-2005: synthesis and future directions. Science. 315:612–7.

Brand, LE, Sunda, W, Guillard RRL (1981) A method for the rapid and precise determination of acclimated phytoplankton reproduction rates. J. Phytoplankton Res. 3: 193-201.

Bruckner CG, Kroth PG (2009) Protocols for the Removal of Bacteria From Freshwater Benthic Diatom Cultures. J. Phycol. 45:981–6.

Brzezinski, MA, CJ Pride, VM Franck, DM Sigman, JL Sarmiento, K Matsumoto, N Gruber, GH Rau, KH Coale (2002) A switch from $Si(OH)_4$ to NO_3^- depletion in the glacial Southern Ocean. Geophys. Res. Lett. 29. doi: 10.1029/2001GL014349

Cheng Z, Li K, Hammad LA, Karty JA, Bauer CE (2014) Vitamin B_{12} regulates photosystem gene expression via the CrtJ antirepressor AerR in Rhodobacter capsulatus. Mol. Microbiol. 91:649–64.

Church MJ, Hutchins DA, Ducklow HW (2000) Limitation of bacterial growth by dissolved organic matter and iron in the Southern Ocean. Appl. Environ. Microbiol. 66: 455-466.

Croft MT, Lawrence AD, Raux-Deery E, Warren MJ, Smith AG (2005) Algae acquire vitamin B_{12} through a symbiotic relationship with bacteria. Nature. 438:90–3.

Croft MT, Warren MJ, Smith AG (2006) Algae need their vitamins. Eukaryot. Cell. 5:1175–83.

Davey M, RJ Geider (2001) Impact of iron limitation on the photosynthetic apparatus of the diatom Chaetoceros muelleri (Bacillariophyceae). J. Phycol. 37: 987-1000.

De Baar HJW, Boyd PW, Coale KH, Landry MR, Tsuda A, et al. (2005) Synthesis of iron fertilization experiments: From the iron age in the age of enlightenment. J. Geophys. Res.: Oceans 110: C09S16.

Dorrell RG, AG Smith (2011) Do red and green make brown?: perspectives on plastid acquisitions within chromalveolates. Euk. Cell 10: 856-868.

Doxey AC, Kurtz DA, Lynch MDJ, Sauder LA, Neufeld JD (2014) Aquatic metagenomes implicate Thaumarchaeota in global cobalamin production. ISME 2014: 1-11.

Droop MR (2007) Vitamins, phytoplankton and bacteria: symbiosis or scavenging? J. Plankton Res. 29**:** 107–113.

Doucette GJ, PJ Harrison (1990) Some effects of iron and nitrogen stress on the red tide dinoflagellate *Gymnodinium sanguineneum*. Mar. Ecol. Prog. Ser. 62: 293-306

Edgar RC (2004) MUSCLE: a multiple sequence alignment method with reduced time and space complexity. BMC Bioinformatics 5: 1-19.

Gobler C, Norman C, Panzeca C, Taylor G, Sañudo-Wilhelmy S (2007) Effect of B-vitamins (B_1, B_{12}) and inorganic nutrients on algal bloom dynamics in a coastal ecosystem. Aquat. Microb. Ecol. 49:181–94.

Gonzalez JC, Banerjee RV, Huang S, Sumner JS, Matthews RG (1992) Comparison of Cobalamin-Independent and Cobalamin-Dependent Methionine Synthases from Escherichia coli: Two solutions to the same chemical problem. Biogeochemistry. 31:6045–56.

Greene RM, Geider RJ, Falkowski PG (1991) Effect of iron limitation on photosynthesis in a marine diatom. Limnology and Oceanography 36:1772-1782.

Greene RM, Geider RJ, Kolber ZS, PG Falkowski (1992) Iron induced changes in light harvesting and photochemical energy conversion processes in eukaryotic marine algae. Plant Physiol 100: 565-575.

Grossart HP, Levold F, Allgaier M, Simon M, Brinkhoff T (2005) Marine diatom species harbour distinct bacterial communities. Environ. Microbiol. 7:860–73.

Helliwell KE, Wheeler GL, Leptos KC, Goldstein RE, Smith AG (2011). Insights into the evolution of vitamin B12 auxotrophy from sequenced algal genomes. Mol. Biol. Evol. 28:2921–33.

Helliwell KE, Wheeler GL, Smith AG (2013) Widespread decay of vitamin-related pathways: coincidence or consequence? Trends Genet. 29:469–78.

Helliwell KE, S Collins, E Kazamia, S Purton, GL Wheeler, A Smith (2015) Fundamental shift in vitamin B_{12} eco-physiology of a model alga demonstrated by experimental evolution. ISME. 9: 1446-1455.

Hoffbrand AV, Weir DG (2001). The history of folic acid. Br. J. Haematol. 113 (3): 579–89.

Hoppe CJM, Hassler CS, Payne CD, Tortell PD, Rost B, Trimborn S (2013) Iron limitation modulates ocean acidification effects on Southern Ocean phytoplankton communities. PLoS ONE 8: e79890.

Hutchins DA (1995) Iron and the marine phytoplankton community. Phycological Research 11:1-49.

Hutchinson GE (1961) The paradox of the plankton. The American Naturalist 95: 137-145.

Kaczmarska I, Ehrman JM, Bates SS, Green DH, Leger C, Harris J (2005) Diversity and distribution of epibiotic bacteria on *Pseudo-nitzschia multiseries* (Bacillariophyceae) in culture, and comparison with those on diatoms in native seawater. Harmful Algae 4:725–741.

Kazamia E, Czesnick H, Nguyen TT, Van Croft MT, Sherwood E, Sasso S, Hodson SJ, et al. (2012) Mutualistic interactions between vitamin B_{12} -dependent algae and heterotrophic bacteria exhibit regulation. Environ. Microbiol. 14:1466–76.

King AL, Sañudo-Wilhelmy SA, Leblanc K, Hutchins DA, Fu F (2011) CO_2 and vitamin B_{12} interactions determine bioactive trace metal requirements of a subarctic Pacific diatom. ISME J. 5:1388–96.

Kirchman DL, Moran XAG, Ducklow H (2009) Microbial growth in the polar oceans – role of temperature and potential impact of climate change. Nature Rev Microbiol 7: 451-459.

Kitajima M, Butler WL (1975) Quenching of chlorophyll fluorescence and primary photochemistry in chloroplasts by dimothymoquinone. Biochim et Biophys Acta 376: 105-115.

Klunder MB, Bauch D, Laan P, de Baar HJW, van Heuven S, Ober S (2012) Dissolved iron in the Arctic shelf seas and surface waters of the central Arctic Ocean: Impact of Arctic river water and ice-melt. Journal of Geophysical Research: Oceans 117:C01027.

Koch, F., Alejandra Marcoval, M., Panzeca, C., Bruland, K.W., Sañudo-Wilhelmy, S. a. & Gobler, C.J. 2011. The effect of vitamin B12 on phytoplankton growth and community structure in the Gulf of Alaska. *Limnol. Oceanogr.* 56:1023–34.

Kooistra, W.H.C.F., Sarno, D., Balzano, S., Gu, H., Anderson, R.A. & Zingone, A. 2008. Global diversity and biogeography of Skeletonema species (Bacillariophyta). *Protist* 159: 177-193.

Lohan MC, Bruland KW (2008) Elevated Fe(II) and dissolved Fe in hypoxic shelf waters off Oregon and Washington: An enhanced source of iron to coastal upwelling regimes. Environmental Science & Technology 42:6462-6468.

Lohmann A, Schottler MA, Brehelin C, Kessler F, Bock R, et al. (2006) Deficiency in phylloquinone (vitamin K_1) methylation affects prenyl quinone distribution, photosystem I

abundance, and anthocyanin accumulation in the Arabidopsis AtmenG mutant. J Biol Chem 281: 40461–40472.

Lundholm N, Daugbjerg N, Moestrup Ø (2011) Phylogeny of the Bacillariaceae with emphasis on the genus Pseudo-nitzschia (Bacillariophyceae) based on partial LSU rDNA. Eur J Phycol 37: 115-134.

Mahowald NM, Baker AR, Bergametti G, Brooks N, Duce RA, Jickells TD, Kubilay N, Prospero JM, Tegen I (2005) Atmospheric global dust cycle and iron inputs to the ocean. Global Biogeochemical Cycles 19:GB4025.

Malin G, Turner SM, Liss PS (1992) Sulfur: The plankton/climate connection. Journal of Phycology 28 (5): 590–597.

Marchetti A, Lundholm N, Kotaki Y, Hubbard K, Harrison PJ, et al. (2008) Identification and assessment of domoic acid production in oceanic *Pseudo-nitzschia* (Bacillariophyceae) from iron-limited waters in the NE Subarctic Pacific. J. Phycol. 44:650-661.

Marchetti A, Schruth DM, Durkin CA, Parker MS, Kodner RB, et al. (2012) Comparative metatranscriptomics identifies molecular bases for the physiological responses of phytoplankton to varying iron availability. PNAS 109: E317-E325.

Matthews RG, Smith AE, Zhou ZS, Taurog RE, Bandarian V, Evans JC, Ludwig M (2003) Cobalamin-Dependent and Cobalamin-Independent Methionine Synthases: Are There Two Solutions to the Same Chemical Problem?. Helvetica Chimica Acta 86 (12): 3939

Medlin LK, Kaczmarska I (2004) Evolution of the diatoms: V. Morphological and cytological support for the major clades and a taxonomic revision. J. Phycol. 43: 245-270.

Menzel DW, JP Spaeth (1962) Occurrence of vitamin B_{12} in the Sargasso Sea. Limnol. and Oceanogr. 7**:** 151–154.

Moore JK, Braucher O (2008) Sedimentary and mineral dust sources of dissolved iron to the world ocean. Biogeosciences 5:631-656.

Nelson DM, P Tréguer, MA Brzezinski, A Leynaert, B Quéguiner. (1995) Production and dissolution of biogenic silica in the ocean: Revised global estimates, comparison with regional data and relationship to biogenic sedimentation. Global Biogeochem. Cycles 9: 359. doi: 10.1029/95GB01070

Noble RT, Fuhrman JA (1998) Use of SYBR Green I for rapid epifluorescence counts of marine viruses and bacteria. Aquat. Microb. Ecol. 14: 113-118.

O'Brien EJ, Lerman JA, Chang RL, Hyduke DR, Palsson BØ (2013) Genome-scale models of metabolism and gene expression extend and refine growth phenotype prediction. Mol. Sys. Biol. 9: 693.

Panzeca C, Tovar-Sanchez A, Agusti S, Reche I, Duarte M, et al. (2006) B vitamins as regulators of phytoplankton dynamics. EOS 87**:** 593–596.

Panzeca C, A Beck, K Leblanc, G Taylor, D Hutchins, S Sañudo-Wilhelmy (2008), Potential cobalt limitation of vitamin B_{12} synthesis in the North Atlantic Ocean, Global Biogeochem. Cycles, 22, GB2029.

Panzeca C, Beck AJ, Tovar-sanchez A, Segovia-zavala J, Taylor GT, Gobler CJ, Sañudo-Wilhelmy SA (2009) Distributions of dissolved vitamin B_{12} and Co in coastal and open-ocean environments. Estuar. Coast. Shelf Sci. 85:223–30.

Parfrey LW, J Grant, YI Tekle, E Lasek-Nesselquist, HG Morrison, et al. (2010) Broadly sampled multigene analyses yield a well-resolved eukaryotic tree of life. Syst. Biol. 59: 1-16.

Pejchal R, Ludwig ML (2005) Cobalamin-Independent Methionine Synthase (MetE): A Face-to-Face Double Barrel That Evolved by Gene Duplication. PLOS Biol. 3:254–65.

Price NM, Harrison GI, Hering JG, Hudson RJ, Nirel PMV, et al. (1988/89) Preparation and chemistry of the artificial algal culture medium Aquil. Biol. Ocean. 6: 443-461.

Raiswell R, Benning L, Tranter M, Tulaczyk S (2008) Bioavailable iron in the Southern Ocean: the significance of the iceberg conveyor belt. Geochemical Transactions 9:7.

Raven JA (1988) The iron and molybdenum use efficiencies of plant growth with different energy, carbon and nitrogen sources. New Phytologist 1988:279-287.

Raven JA (1990) Predictions of Mn and Fe use efficiencies of phototrophic growth as a function of light availability for growth and of C assimilation pathway. New Phytol 116:1-18

Rodionov DA, AG Vitreschak, AA Mironov, MS Gelfand (2003) Comparative genomics of the vitamin B_{12} metabolism and regulation in prokaryotes. J. Biol. Chem. 278: 41148-41159. doi: 10.1074/jbc.M305837200

Rue EL, Bruland KW (1995) Complexation of iron (III) by natural organic ligands in the Central North Pacific as determined by a new competitive ligand equilibration/adsorptive cathodic stripping voltammetric method. Marine Chemistry 50:117-138.

Sañudo-Wilhelmy SA, Gobler CJ, Okbamichael M, Taylor GT (2006) Regulation of phytoplankton dynamics by vitamin B_{12}. Geophys. Res. Let. 33: L04604.

Sañudo-Wilhelmy SA, Cutter LS, Durazo R, Smail EA, Gómez-Consarnau L, Webb EA, Prokopenko MG, et al. (2012) Multiple B-vitamin depletion in large areas of the coastal ocean. Proc. Natl. Acad. Sci. U. S. A. 109:14041–5.

Sañudo-Wilhelmy SA, Gómez-Consarnau L, Suffridge C, Webb EA (2014) The role of B vitamins in marine biogeochemistry. Ann. Rev. Mar. Sci. 6:339–67.

Shishlyannikov SM, Zakharova YR, Volokitina NA, Mikhailov IS, Petrova DP, Likhoshway YV (2011) A procedure for establishing an axenic culture of the diatom Synedra acus subsp. radians (Kütz.) Skabibitsch. from Lake Baikal Limnol. Oceanogr. Methods. 9:478–84.

Smetacek V, Klaas C, Strass VH, Assmy P, Montresor M, Cisewski B, Savoye N, et al. (2012) Deep carbon export from a Southern Ocean iron-fertilized diatom bloom. Nature. 487:313–9.

Sorhannus U (2007) A nuclear-encoded small-subunit ribosomal RNA timescale for diatom evolution. Mar. Micropaleo. 65: 1-12.

Suggett DJ, CM Moore, AE Hickman, RJ Geider (2009) Interpretation of fast repetition rate (FRR) fluorescence: signatures of phytoplankton community structure versus physiological state. Mar. Ecol. Prog. Ser. 376: 1-19.

Timmermans KR, Stolte W, de Baar HJW (1994) Ironmediated effects on nitrate reductase in marine phytoplankton. Mar. Biol. 121: 389–396.

Timmermans KR, et al. (1998) Iron limitation in the Pacific region of the Southern Ocean: Evidence from enrichment bioassays. Mar. Ecol. Prog. Ser. 166: 27–41.

Takeda S (1998) Influence of iron availability on nutrient consumption ratio of diatoms in oceanic waters. Nature 393:774-777.

Wells ML, Price NM, Bruland KW (1995) Iron chemistry in seawater and its relationship to phytoplankton - a workshop report. Mar Chem 48:157-182.

Wetz MS, Hales B, Chase Z, Wheeler PA, Whitney MM (2006) Riverine input of macronutrients, iron, and organic matter to the coastal ocean off Oregon, USA, during the winter. Limnology and Oceanography 51:2221-2231.